INTERNATIONAL JOURNAL OF
NUMERICAL ANALYSIS AND MODELING
Volume 21, Number 6, Pages 793–821

doi: 10.4208/ijnam2024-1032

SIXTH-ORDER COMPACT DIFFERENCING WITH STAGGERED BOUNDARY SCHEMES AND 3(2) BOGACKI-SHAMPINE PAIRS FOR PRICING FREE-BOUNDARY OPTIONS

CHINONSO NWANKWO* AND WEIZHONG DAI

Abstract. We propose a stable sixth-order compact finite difference scheme coupled with a fifth-order staggered boundary scheme and the Runge-Kutta adaptive time stepping based on 3(2) Bogacki-Shampine pairs for pricing American options. To compute the free-boundary simultaneously and precisely with the option value and Greeks, we introduce a logarithmic Landau transformation and then remove the convective term in the pricing model by introducing the delta sensitivity, so that an efficient sixth-order compact scheme can be easily implemented. The main challenge in coupling the sixth order compact scheme in discrete form is to efficiently account for the near-boundary scheme. In this study, we introduce novel fifth and sixth-order Dirichlet near-boundary schemes that are suitable for solving our model. The optimal exercise boundary and other boundary values are approximated using a high-order analytical approximation that is obtained from a novel fifth-order staggered boundary scheme. Furthermore, we investigate the smoothness of the first and second-order derivatives of the optimal exercise boundary which is obtained from the high-order analytical approximation. Coupled with the adaptive time integration method, the interior values are then approximated using the sixth order compact schemes. As such, the expected convergence rate is reasonably achieved, and the present numerical scheme is very fast in computation and gives highly accurate solutions with very coarse grids.

Key words. Sixth-order compact finite difference, 3(2) Bogacki and Shampine pairs, Dirichlet and Neumann boundary conditions, options price, Delta sensitivity, optimal exercise boundary.

1. Introduction

Under risk neutral probability, the model governing the American style put options value $P(S,t)$ and the optimal exercise boundary $s_f(t)$ can be expressed as

$$\frac{\partial P(S,t)}{\partial t} - \frac{\sigma}{2}\frac{\partial^2 P(S,t)}{\partial S^2} - r\frac{\partial P(S,t)}{\partial S} + rP(S,t) = 0, \quad S > s_f(t), \quad t > 0; \tag{1}$$

$$P(S,t) = E - S, \qquad S < s_f(t); \tag{2}$$

$$P(s_f(t),t) = E - s_f(t), \qquad \frac{\partial P(s_f(t),t)}{\partial S} = -1; \tag{3}$$

$$P(\infty,t) = 0, \qquad \frac{\partial P(\infty,t)}{\partial S} = 0; \tag{4}$$

$$s_f(0) = E, \qquad P(S,0) = \max(E-S,0). \tag{5}$$

Here, S is the asset price, T is the time to maturity E is the strike price, σ is the volatility, and r is the interest rate. It can be seen that the above model is a free boundary problem since $s_f(t)$ varies with time. There is no closed-form solution for this model and therefore, it must be solved using numerical or semi-analytical methods. The solution framework for the above model can be formulated as a linear complementary problem, with a penalty method or front-fixing approach. However,

Received by the editors on October 9, 2023 and, accepted on March 29, 2024.
2000 *Mathematics Subject Classification.* 35Q91, 65M06, 65M22, 65N50.
*Corresponding author.

in a linear complementary framework also known as variational inequality and the penalty method, constraints are imposed and it has been shown that the obtained optimal exercise boundary is not very accurate. In the front-fixing approach [38], one may apply the Landau transformation

$$x = \ln \frac{S}{s_f(t)}, \qquad P(e^x s_f(t), t) = U(x,t), \tag{6}$$

to (6) and obtain a fixed free-boundary equation as follows:

$$\frac{\partial U(x,t)}{\partial t} - \frac{\sigma^2}{2}\frac{\partial^2 U(x,t)}{\partial x^2} - \xi_t \frac{\partial U(x,t)}{\partial x} + rU(x,t) = 0, \qquad x > 0; \tag{7}$$

where

$$\xi_t = r - \frac{s_f'(t)}{s_f(t)} - \frac{\sigma^2}{2}. \tag{8}$$

Although the free-boundary is now fixed at $x = 0$, it is worth observing that (7) becomes a nonlinear partial differential equation with a singular coefficient. This is because the derivative of the optimal exercise boundary involved in the coefficient of the convective term is not continuous at payoff. This irregularity presents a source of non-smoothness in the model and the convective term could further introduce substantial errors when using numerical approximation. To remove $\frac{\partial U(x,t)}{\partial x}$, we in this study introduce the delta sensitivity $W(x,t)$ as

$$W(x,t) = \frac{\partial U(x,t)}{\partial x}. \tag{9}$$

Thus, we obtain a system of two fixed-free boundary partial differential equations (PDEs) for the option value and delta sensitivity that is suitable for implementing an efficient sixth-order compact scheme as follows:

$$\frac{\partial U(x,t)}{\partial t} - \frac{\sigma^2}{2}\frac{\partial^2 U(x,t)}{\partial x^2} - \xi_t W(x,t) + rU(x,t) = 0, \qquad x > 0; \tag{10}$$

$$\frac{\partial W(x,t)}{\partial t} - \frac{\sigma^2}{2}\frac{\partial^2 W(x,t)}{\partial x^2} - \xi_t \frac{\partial^2 U(x,t)}{\partial x^2} + rW(x,t) = 0, \qquad x > 0; \tag{11}$$

$$U(x,t) = E - e^x s_f(t), \qquad W(x,t) = -e^x s_f(t), \qquad x \le 0; \tag{12}$$

with initial and boundary conditions:

$$U(0,t) = E - s_f(t), \qquad W(0,t) = -s_f(t); \tag{13}$$

$$U(\infty,t) \cong 0, \qquad W(\infty,t) \cong 0; \tag{14}$$

$$U(x,0) = 0, \qquad W(x,0) = 0, \qquad x > 0; \tag{15}$$

$$U(0,0) = 0, \qquad \lim_{x \to 0^+} W(x,0) = 0. \tag{16}$$

Under an assumption of sufficient smoothness, a high-order numerical scheme can be used to obtain a more accurate numerical solution with very coarse grids. This feature could be beneficial in saving computational time and improving complexity in high dimensional context. However, the non-smoothness in the transformed model hampers this possibility [1, 6, 22, 33]. Several authors have tried to implement high-order numerical scheme for solving American options using the front-fixing approach. Hajipour and Malek [15] implemented an efficient fifth-order WENO-BDF3 scheme for solving the American options but only recovered a second-order accurate solution. Tangman et al. [33] implemented a fourth-order numerical scheme

with coordinate transformation. However, they could not recover the convergence rate that is in good agreement with the theoretical convergence rate. Ballestra [1], who used a second-order numerical scheme, recovered a high order convergence rate by implementing a time-variable transformation and Richardson extrapolation. Nwankwo and Dai [25, 26, 27] improved the non-smoothness in the transformed model using a high-order analytical approximation. They further implemented a fourth-order compact finite difference scheme and recovered a convergence rate that is in good agreement with the theoretical convergence rate.

Recently, Sari and Gulen [29] implemented a sixth-order finite difference scheme for pricing the American options model using the front-fixing approach. However, they did not address the non-smoothness in the model, and approximated the optimal exercise boundary and near-boundary points using the approach of Company et al. [9] which is, at most, second-order accurate in space. This approach could reduce the performance of the sixth-order finite difference scheme. Thus, Yambangwai and Moshkin [39] described approaches for improving low-order accurate Dirichlet and Neumann boundary schemes to be consistent with high-order interior schemes using deferred correction techniques. Here, we further acknowledge the recent work of Wang et al. [35] where they implemented a deferred correction method for improving and increasing accuracy in American options using the penalty method.

In this research work, we are particularly interested in the precise computation of the optimal exercise boundary and its derivatives. This is because the left boundary values are not exact. They are rather obtained from the numerical solution of the optimal exercise boundary at $x = 0$. Hence, a precise approximation of the optimal exercise boundary could enable us to obtain a more accurate numerical solution of the asset option and delta sensitivity. Furthermore, the coefficient of the convective term in the transformed model involves the derivative of the optimal exercise boundary. It entails a strong need to further obtain a more precise solution of the first-order derivative of the optimal exercise boundary. The question that remains is at what cost can we achieve these possibilities. For the above purpose, we propose a stable, fast, and very accurate sixth-order compact finite difference scheme coupled withs third-order adaptive time stepping based on 3(2) Bogacki and Shampine pairs [2] for pricing American options using a front-fixing approach. Here, we pay more attention to the boundary and near-boundary schemes for approximating the optimal exercise boundary and the boundary values of both the asset option and the delta sensitivity. We first derive novel fifth and sixth-order Dirichlet near-boundary schemes that are suitable for approximating our model. We then construct a dynamic fifth-order staggered boundary scheme for approximating the optimal exercise boundary and the boundary values. As such, a highly accurate numerical solution can be obtained using a very coarse grid. The rest of the paper is organized as follows. In section 2, we present the proposed sixth-order compact finite difference for solving our model. In section 3, we demonstrate the performance of our proposed method through numerical examples and comparison. We then conclude in section 4.

2. Compact Finite Difference Scheme

Our computational domain is defined on $[0, x_{\max}] \times [0, T]$. The asset price domain $[0, x_{\max}]$ is a truncated domain that replaces the semi-positive infinite domain $[0, \infty)$. It has been shown that only negligible error is introduced [9] because the options value vanishes rapidly as x increases. Here, we implement an adaptive time

stepping on the time domain. For the space domain, if we denote x_j as a grid point, h as the step size, and n_x as the number of the grid points, then we obtain

$$x_i = ih, \qquad h = \frac{x_{\max}}{n_x}, \qquad i = 0, 1, \cdots, n_x. \tag{17}$$

We denote the numerical solution of the optimal exercise boundary, asset options, and delta sensitivity as s_f^n, u_i^n, and w_i^n, respectively.

2.1. Sixth order compact finite difference scheme. We first present a sixth-order compact finite difference scheme for approximating the option value, delta sensitivity, and optimal exercise boundary simultaneously. From (13), one may see that there exists a relationship between the optimal exercise boundary and the boundary values of the asset option and delta sensitivity. Hence, we can compute the boundary values from the optimal exercise boundary. To this end, we introduce new fifth- and sixth-order near-boundary schemes as follows:

$$\begin{aligned} f(x_2,\cdot) =& f(x_1,\cdot) + h\frac{\partial f(x_1,\cdot)}{\partial x} + \frac{h^2}{2!}\frac{\partial^2 f(x_1,\cdot)}{\partial x^2} + \frac{h^3}{3!}\frac{\partial^3 f(x_1,\cdot)}{\partial x^3} + \frac{h^4}{4!}\frac{\partial^4 f(x_1,\cdot)}{\partial x^4} \\ &+ \frac{h^5}{5!}\frac{\partial^5 f(x_1,\cdot)}{\partial x^5} + \frac{h^6}{6!}\frac{\partial^6 f(x_1,\cdot)}{\partial x^6} + \frac{h^7}{7!}\frac{\partial^7 f(x_1,\cdot)}{\partial x^7} + O(h^8), \end{aligned} \tag{18}$$

$$\begin{aligned} f(x_0,\cdot) =& f(x_1,\cdot) - h\frac{\partial f(x_1,\cdot)}{\partial x} + \frac{h^2}{2!}\frac{\partial^2 f(x_1,\cdot)}{\partial x^2} - \frac{h^3}{3!}\frac{\partial^3 f(x_1,\cdot)}{\partial x^3} + \frac{h^4}{4!}\frac{\partial^4 f(x_1,\cdot)}{\partial x^4} \\ &- \frac{h^5}{5!}\frac{\partial^5 f(x_1,\cdot)}{\partial x^5} + \frac{h^6}{6!}\frac{\partial^6 f(x_1,\cdot)}{\partial x^6} - \frac{h^7}{7!}\frac{\partial^7 f(x_1,\cdot)}{\partial x^7} + O(h^8). \end{aligned} \tag{19}$$

Adding them together and then dividing it by h^2 gives

$$\begin{aligned} &\frac{f(x_0,\cdot) - 2f(x_1,\cdot) + f(x_2,\cdot)}{h^2} \\ =& \frac{\partial^2 f(x_1,\cdot)}{\partial x^2} + \frac{2h^2}{4!}\frac{\partial^4 f(x_1,\cdot)}{\partial x^4} + \frac{2h^4}{6!}\frac{\partial^6 f(x_1,\cdot)}{\partial x^6} + O(h^6). \end{aligned} \tag{20}$$

Here, if we substitute the following forward finite difference scheme into (20)

$$h^2\frac{\partial^4 f(x_1,\cdot)}{\partial x^4} = 2\frac{\partial^2 f(x_1,\cdot)}{\partial x^2} - 5\frac{\partial^2 f(x_2,\cdot)}{\partial x^2} + 4\frac{\partial^2 f(x_3,\cdot)}{\partial x^2} - \frac{\partial^2 f(x_4,\cdot)}{\partial x^2} + O(h^4), \tag{21}$$

we obtain

$$\begin{aligned} &14\frac{\partial^2 f(x_1,\cdot)}{\partial x^2} - 5\frac{\partial^2 f(x_2,\cdot)}{\partial x^2} + 4\frac{\partial^2 f(x_3,\cdot)}{\partial x^2} - \frac{\partial^2 f(x_4,\cdot)}{\partial x^2} \\ =& \frac{12}{h^2}\frac{f(x_0,\cdot) - 2f(x_1,\cdot) + f(x_2,\cdot)}{h^2} + O(h^4). \end{aligned} \tag{22}$$

The above fourth-order scheme is the same as the one presented in the work of Zhao [41] and Zhao et al. [40, 42] from which we draw some inspiration to extend beyond fourth-order accuracy. Zhao et al. [40, 42] also presented several fourth-order Dirichlet and Neumann near-boundary schemes that are more suitable for approximating partial differential equations and partial integro differential equations arising in the options pricing models. However, when we approximated our model using the sixth-order combined compact scheme presented in [41], we observed that the numerical accuracy deteriorates as the step size gets smaller.

Notwithstanding, we borrowed insight from their other works [40, 42] to obtain novel fifth and sixth-order Dirichlet near-boundary schemes. To achieve at least fifth order accuracy near the boundary for $i = 1$, we consider the following two forward finite difference approximations

$$h^2\frac{\partial^4 f(x_1,\cdot)}{\partial x^4} = \frac{35}{12}\frac{\partial^2 f(x_1,\cdot)}{\partial x^2} - \frac{26}{3}\frac{\partial^2 f(x_2,\cdot)}{\partial x^2} + \frac{19}{2}\frac{\partial^2 f(x_3,\cdot)}{\partial x^2}$$

$$- \frac{14}{3}\frac{\partial^2 f(x_4,\cdot)}{\partial x^2} + \frac{11}{3}\frac{\partial^2 f(x_5,\cdot)}{\partial x^2} + O(h^5), \tag{23}$$

$$h^2\frac{\partial^6 f(x_1,\cdot)}{\partial x^6} = \frac{\partial^2 f(x_1,\cdot)}{\partial x^2} - 4\frac{\partial^2 f(x_2,\cdot)}{\partial x^2} + 6\frac{\partial^2 f(x_3,\cdot)}{\partial x^2}$$

$$- 4\frac{\partial^2 f(x_4,\cdot)}{\partial x^2} + \frac{\partial^2 f(x_5,\cdot)}{\partial x^2} + O(h^5). \tag{24}$$

Substituting (23) and (24) into (20), we obtain

$$\frac{897}{60}\frac{\partial^2 f(x_1,\cdot)}{\partial x^2} - \frac{528}{60}\frac{\partial^2 f(x_2,\cdot)}{\partial x^2} + \frac{582}{60}\frac{\partial^2 f(x_3,\cdot)}{\partial x^2} - \frac{288}{60}\frac{\partial^2 f(x_4,\cdot)}{\partial x^2}$$

$$+ \frac{57}{60}\frac{\partial^2 f(x_5,\cdot)}{\partial x^2} = \frac{12}{h^2}\frac{f(x_0,\cdot) - 2f(x_1,\cdot) + f(x_2,\cdot)}{h^2} + O(h^5). \tag{25}$$

Furthermore, to achieve sixth-order accuracy near the boundary for $i = 1$, we consider the following forward finite difference approximation

$$h^2\frac{\partial^4 f(x_1,\cdot)}{\partial x^4} = \frac{15}{4}\frac{\partial^2 f(x_1,\cdot)}{\partial x^2} - \frac{77}{6}\frac{\partial^2 f(x_2,\cdot)}{\partial x^2} + \frac{107}{6}\frac{\partial^2 f(x_3,\cdot)}{\partial x^2}$$

$$- 13\frac{\partial^2 f(x_4,\cdot)}{\partial x^2} + \frac{61}{12}\frac{\partial^2 f(x_5,\cdot)}{\partial x^2} - \frac{5}{6}\frac{\partial^2 f(x_6,\cdot)}{\partial x^2} + O(h^6), \tag{26}$$

$$h^2\frac{\partial^6 f(x_1,\cdot)}{\partial x^6} = 3\frac{\partial^2 f(x_1,\cdot)}{\partial x^2} - 14\frac{\partial^2 f(x_2,\cdot)}{\partial x^2} + 26\frac{\partial^2 f(x_3,\cdot)}{\partial x^2}$$

$$- 24\frac{\partial^2 f(x_4,\cdot)}{\partial x^2} + 11\frac{\partial^2 f(x_5,\cdot)}{\partial x^2} - 2\frac{\partial^2 f(x_6,\cdot)}{\partial x^2} + O(h^6). \tag{27}$$

Substituting (26) and (27) into (20), we obtain

$$\frac{1902}{120}\frac{\partial^2 f(x_1,\cdot)}{\partial x^2} - \frac{1596}{120}\frac{\partial^2 f(x_2,\cdot)}{\partial x^2} + \frac{2244}{120}\frac{\partial^2 f(x_3,\cdot)}{\partial x^2} - \frac{1656}{120}\frac{\partial^2 f(x_4,\cdot)}{\partial x^2}$$

$$+ \frac{654}{120}\frac{\partial^2 f(x_5,\cdot)}{\partial x^2} - \frac{108}{120}\frac{\partial^2 f(x_6,\cdot)}{\partial x^2} = \frac{12}{h^2}\frac{f(x_0,\cdot) - 2f(x_1,\cdot) + f(x_2,\cdot)}{h^2} + O(h^6). \tag{28}$$

Subsequently, for $i = n_x - 1$, we have

$$\begin{aligned}\frac{897}{60}\frac{\partial^2 f(x_{n_x-1},\cdot)}{\partial x^2} - \frac{528}{60}\frac{\partial^2 f(x_{n_x-2},\cdot)}{\partial x^2} + \frac{582}{60}\frac{\partial^2 f(x_{n_x-3},\cdot)}{\partial x^2} \\ - \frac{288}{60}\frac{\partial^2 f(x_{n_x-4},\cdot)}{\partial x^2} + \frac{57}{60}\frac{\partial^2 f(x_{n_x-5},\cdot)}{\partial x^2} \\ = \frac{12}{h^2}\frac{f(x_{n_x-2},\cdot) - 2f(x_{n_x-1},\cdot) + f(x_{n_x-1},\cdot)}{h^2} + O(h^5), \end{aligned} \tag{29}$$

$$\begin{aligned}\frac{1902}{120}\frac{\partial^2 f(x_{n_x-1},\cdot)}{\partial x^2} - \frac{1596}{120}\frac{\partial^2 f(x_{n_x-2},\cdot)}{\partial x^2} + \frac{2244}{120}\frac{\partial^2 f(x_{n_x-3},\cdot)}{\partial x^2} \\ - \frac{1656}{120}\frac{\partial^2 f(x_{n_x-4},\cdot)}{\partial x^2} + \frac{654}{120}\frac{\partial^2 f(x_{n_x-5},\cdot)}{\partial x^2} - \frac{108}{120}\frac{\partial^2 f(x_6,\cdot)}{\partial x^2} \\ = \frac{12}{h^2}\frac{f(x_{n_x-2},\cdot) - 2f(x_{n_x-1},\cdot) + f(x_{n_x},\cdot)}{h^2} + O(h^6). \end{aligned} \tag{30}$$

with $f(x_{n_x},\cdot) = 0$ due to the far-right boundary. On the other hand, for $i = 2,\cdots,n_x-2$, we employ the well-known sixth-order compact scheme

$$\begin{aligned}&\frac{2}{11}\frac{\partial^2 f(x_{i-1},\cdot)}{\partial x^2} + \frac{\partial^2 f(x_i,\cdot)}{\partial x^2} + \frac{2}{11}\frac{\partial^2 f(x_{i+1},\cdot)}{\partial x^2} \\ &= \frac{3}{44h^2}f(x_{i-2},\cdot) + \frac{12}{11h^2}f(x_{i-1},\cdot) - \frac{51}{22h^2}f(x_i,\cdot) + \frac{12}{11h^2}f(x_{i+1},\cdot) \\ &+ \frac{3}{44h^2}f(x_{i+2},\cdot) + O(h^6). \end{aligned} \tag{31}$$

In matrix-vector form, the discrete system of two equations is presented as follows:

$$B_{5,6}\mathbf{u}'' = A_h\mathbf{u} + \mathbf{f}_{u,h}, \qquad B_{5,6}\mathbf{w}'' = A_h\mathbf{w} + \mathbf{f}_{w,h}. \tag{32}$$

Here, $B_{5,6} \in \{B_5, B_6\}$ and

$$A_h = \frac{1}{h^2}\begin{bmatrix} -24 & 12 & 0 & 0 & 0 & 0 & \cdots & 0 & 0 \\ \frac{12}{11} & -\frac{51}{22} & \frac{12}{11} & \frac{3}{44} & 0 & 0 & \cdots & 0 & 0 \\ \frac{3}{44} & \frac{12}{11} & -\frac{51}{22} & \frac{12}{11} & \frac{3}{44} & 0 & \cdots & 0 & 0 \\ 0 & \frac{3}{44} & \frac{12}{11} & -\frac{51}{22} & \frac{12}{11} & \frac{3}{44} & \cdots & 0 & 0 \\ \vdots & \vdots & \vdots & \ddots & \ddots & \ddots & \vdots & \vdots & \vdots \\ 0 & 0 & \cdots & \frac{3}{44} & \frac{12}{11} & -\frac{51}{22} & \frac{12}{11} & \frac{3}{44} & 0 \\ 0 & 0 & \cdots & 0 & \frac{3}{44} & \frac{12}{11} & -\frac{51}{22} & \frac{12}{11} & \frac{3}{44} \\ 0 & 0 & \cdots & 0 & 0 & \frac{3}{44} & \frac{12}{11} & -\frac{51}{22} & \frac{12}{11} \\ 0 & 0 & \cdots & 0 & 0 & 0 & 0 & 12 & -24 \end{bmatrix},$$

$$B_5 = \begin{bmatrix} \frac{897}{60} & -\frac{528}{60} & \frac{582}{60} & -\frac{288}{60} & \frac{57}{60} & 0 & \cdots & 0 & 0 \\ \frac{2}{11} & 1 & \frac{2}{11} & 0 & 0 & 0 & \cdots & 0 & 0 \\ 0 & \frac{2}{11} & 1 & \frac{2}{11} & 0 & 0 & \cdots & 0 & 0 \\ 0 & 0 & \frac{2}{11} & 1 & \frac{2}{11} & 0 & \cdots & 0 & 0 \\ \vdots & \vdots & \vdots & \ddots & \ddots & \ddots & \vdots & \vdots & \vdots \\ 0 & 0 & \cdots & 0 & \frac{2}{11} & 1 & \frac{2}{11} & 0 & 0 \\ 0 & 0 & \cdots & 0 & 0 & \frac{2}{11} & 1 & \frac{2}{11} & 0 \\ 0 & 0 & \cdots & 0 & 0 & 0 & \frac{2}{11} & 1 & \frac{2}{11} \\ 0 & 0 & \cdots & 0 & \frac{57}{60} & -\frac{288}{60} & \frac{582}{60} & -\frac{528}{60} & \frac{897}{60} \end{bmatrix},$$

$$B_6 = \begin{bmatrix} \frac{1902}{120} & -\frac{1596}{120} & \frac{2244}{120} & -\frac{1656}{120} & \frac{654}{120} & -\frac{108}{120} & \cdots & 0 & 0 \\ \frac{2}{11} & 1 & \frac{2}{11} & 0 & 0 & 0 & \cdots & 0 & 0 \\ 0 & \frac{2}{11} & 1 & \frac{2}{11} & 0 & 0 & \cdots & 0 & 0 \\ 0 & 0 & \frac{2}{11} & 1 & \frac{2}{11} & 0 & \cdots & 0 & 0 \\ \vdots & \vdots & \vdots & \ddots & \ddots & \ddots & \vdots & \vdots & \vdots \\ 0 & 0 & \cdots & 0 & \frac{2}{11} & 1 & \frac{2}{11} & 0 & 0 \\ 0 & 0 & \cdots & 0 & 0 & \frac{2}{11} & 1 & \frac{2}{11} & 0 \\ 0 & 0 & \cdots & 0 & 0 & 0 & \frac{2}{11} & 1 & \frac{2}{11} \\ 0 & 0 & \cdots & -\frac{108}{120} & \frac{654}{120} & -\frac{1656}{120} & \frac{2244}{120} & -\frac{1596}{120} & \frac{1902}{120} \end{bmatrix},$$

$$\mathbf{f}_{u,h} = \frac{1}{h^2}\begin{bmatrix} 12u_0^n \\ \frac{3}{44}u_0^n \\ 0 \\ 0 \\ \vdots \\ 0 \\ 0 \\ \frac{3}{44}u_{n_x}^n \\ 12u_{n_x}^n \end{bmatrix}, \qquad \mathbf{f}_{w,h} = \frac{1}{h^2}\begin{bmatrix} 12w_0^n \\ \frac{3}{44}w_0^n \\ 0 \\ 0 \\ \vdots \\ 0 \\ 0 \\ \frac{3}{44}w_{n_x}^n \\ 12w_{n_x}^n \end{bmatrix}.$$

We would love to emphasize that the fourth, fifth and sixth-order Dirichlet near-boundary schemes we derived above are more suitable for our numerical approximation when we compared them with the one in the work of Mehra [24]. Furthermore, it could easily be seen that we have avoided $\frac{\partial^2 f(0,\cdot)}{\partial x^2}$ in the presented schemes. This is a very important feature to observe because of the behavior of the first and second-order derivatives of the option value at the payoff. When we used the sixth order Dirichlet near-boundary scheme in the work of Mehra [24] for approximating our model, we obtained numerical divergence. It is on this notion that our interest was spurred to derive new fifth and sixth-order Dirichlet near-boundary schemes suitable for our discrete system. Further observation reveals that A_h is dependent on h while the entries of the matrix B_5 is constant. However, A_h is diagonally dominant.

2.2. Dynamic and fifth-order staggered exercise boundary scheme. Here, we dynamically construct a fifth-order staggered boundary scheme which will allow us to manipulate how we use grid points arbitrarily near the left boundary when approximating the optimal exercise boundary, and the boundary values of the asset

option and delta sensitivity. To this end, we first introduce the following Taylor series expansion at the left boundary as follows:

$$\begin{aligned} f(h_1,\cdot) =& f(0,\cdot) + a_1\frac{\partial f(0,\cdot)}{\partial x} + a_2\frac{\partial^2 f(0,\cdot)}{\partial x^2} + a_3\frac{\partial^3 f(0,\cdot)}{\partial x^3} + a_4\frac{\partial^4 f(0,\cdot)}{\partial x^4} \\ &+ a_5\frac{\partial^5 f(0,\cdot)}{\partial x^5} + a_6\frac{\partial^6 f(0,\cdot)}{\partial x^6} + a_7\frac{\partial^7 f(0,\cdot)}{\partial x^7} + O(h^8), \end{aligned} \tag{33}$$

$$\begin{aligned} f(h_2,\cdot) =& f(0,\cdot) + b_1\frac{\partial f(0,\cdot)}{\partial x} + b_2\frac{\partial^2 f(0,\cdot)}{\partial x^2} + b_3\frac{\partial^3 f(0,\cdot)}{\partial x^3} + b_4\frac{\partial^4 f(0,\cdot)}{\partial x^4} \\ &+ b_5\frac{\partial^5 f(0,\cdot)}{\partial x^5} + b_6\frac{\partial^6 f(0,\cdot)}{\partial x^6} + b_7\frac{\partial^7 f(0,\cdot)}{\partial x^7} + O(h^8), \end{aligned} \tag{34}$$

$$\begin{aligned} f(h_3,\cdot) =& f(0,\cdot) + c_1\frac{\partial f(0,\cdot)}{\partial x} + c_2\frac{\partial^2 f(0,\cdot)}{\partial x^2} + c_3\frac{\partial^3 f(0,\cdot)}{\partial x^3} + c_4\frac{\partial^4 f(0,\cdot)}{\partial x^4} \\ &+ c_5\frac{\partial^5 f(0,\cdot)}{\partial x^5} + c_6\frac{\partial^6 f(0,\cdot)}{\partial x^6} + c_7\frac{\partial^7 f(0,\cdot)}{\partial x^7} + O(h^8), \end{aligned} \tag{35}$$

$$\begin{aligned} f(h_4,\cdot) =& f(0,\cdot) + d_1\frac{\partial f(0,\cdot)}{\partial x} + d_2\frac{\partial^2 f(0,\cdot)}{\partial x^2} + d_3\frac{\partial^3 f(0,\cdot)}{\partial x^3} + d_4\frac{\partial^4 f(0,\cdot)}{\partial x^4} \\ &+ d_5\frac{\partial^5 f(0,\cdot)}{\partial x^5} + d_6\frac{\partial^6 f(0,\cdot)}{\partial x^6} + d_7\frac{\partial^7 f(0,\cdot)}{\partial x^7} + O(h^8), \end{aligned} \tag{36}$$

$$\begin{aligned} f(h_5,\cdot) =& f(0,\cdot) + e_1\frac{\partial f(0,\cdot)}{\partial x} + e_2\frac{\partial^2 f(0,\cdot)}{\partial x^2} + e_3\frac{\partial^3 f(0,\cdot)}{\partial x^3} + e_4\frac{\partial^4 f(0,\cdot)}{\partial x^4} \\ &+ e_5\frac{\partial^5 f(0,\cdot)}{\partial x^5} + e_6\frac{\partial^6 f(0,\cdot)}{\partial x^6} + e_7\frac{\partial^7 f(0,\cdot)}{\partial x^7} + O(h^8), \end{aligned} \tag{37}$$

where $h_i = \gamma_i h$ and

$$a_i = \frac{\gamma_1^i h^i}{i!}, \qquad b_i = \frac{\gamma_2^i h^i}{i!}, \qquad c_i = \frac{\gamma_3^i h^i}{i!}, \qquad d_i = \frac{\gamma_4^i h^i}{i!}, \qquad e_i = \frac{\gamma_5^i h^i}{i!}. \tag{38}$$

Here, γ_1, γ_2, γ_3, γ_4, and γ_5 are arbitrary and can be varied to control the distribution of the grid points when approximating the optimal exercise boundary. We leverage this feature to manipulate the distribution of grid points around the left boundary when computing the boundary values, hence presenting a high-order dynamic and staggered boundary scheme. Denote

$$i_1 = \frac{b_7}{a_7}, \qquad j_1 = \frac{c_7}{b_7}, \qquad k_1 = \frac{d_7}{c_7}, \qquad l_1 = \frac{e_7}{d_7}. \tag{39}$$

If we multiply (33) by i_1 and subtract it from (34), we obtain

$$i_1 f(h_1,\cdot) - f(h_2,\cdot) = (i_1-1)f(0,\cdot) + (a_1 i_1 - b_1)\frac{\partial f(0,\cdot)}{\partial x} + (a_2 i_2 - b_2)\frac{\partial^2 f(0,\cdot)}{\partial x^2} +$$

$$+ (a_3 i_3 - b_3)\frac{\partial^3 f(0,\cdot)}{\partial x^3} + (a_4 i_4 - b_4)\frac{\partial^4 f(0,\cdot)}{\partial x^4} + (a_5 i_5 - b_5)\frac{\partial^5 f(0,\cdot)}{\partial x^5}$$

$$+ (a_6 i_6 - b_6)\frac{\partial^6 f(0,\cdot)}{\partial x^6} + O(h^8), \tag{40}$$

$$j_1 f(h_2,\cdot) - f(h_3,\cdot) = (j_1-1)f(0,\cdot) + (b_1 j_1 - c_1)\frac{\partial f(0,\cdot)}{\partial x} + (b_2 j_2 - c_2)\frac{\partial^2 f(0,\cdot)}{\partial x^2} +$$

$$+ (b_3 j_3 - c_3)\frac{\partial^3 f(0,\cdot)}{\partial x^3} + (b_4 j_4 - c_4)\frac{\partial^4 f(0,\cdot)}{\partial x^4} + (b_5 j_5 - c_5)\frac{\partial^5 f(0,\cdot)}{\partial x^5}$$

$$+ (b_6 j_6 - c_6)\frac{\partial^6 f(0,\cdot)}{\partial x^6} + O(h^8), \tag{41}$$

$$k_1 f(h_3,\cdot) - f(h_4,\cdot) = (k_1-1)f(0,\cdot) + (c_1 k_1 - d_1)\frac{\partial f(0,\cdot)}{\partial x} + (c_2 k_2 - d_2)\frac{\partial^2 f(0,\cdot)}{\partial x^2} +$$

$$+ (c_3 k_3 - d_3)\frac{\partial^3 f(0,\cdot)}{\partial x^3} + (c_4 k_4 - d_4)\frac{\partial^4 f(0,\cdot)}{\partial x^4} + (c_5 k_5 - d_5)\frac{\partial^5 f(0,\cdot)}{\partial x^5}$$

$$+ (c_6 k_6 - d_6)\frac{\partial^6 f(0,\cdot)}{\partial x^6} + O(h^8), \tag{42}$$

$$l_1 f(h_4,\cdot) - f(h_5,\cdot) = (l_1-1)f(0,\cdot) + (d_1 l_1 - e_1)\frac{\partial f(0,\cdot)}{\partial x} + (d_2 l_2 - e_2)\frac{\partial^2 f(0,\cdot)}{\partial x^2} +$$

$$+ (d_3 l_3 - e_3)\frac{\partial^3 f(0,\cdot)}{\partial x^3} + (d_4 l_4 - e_4)\frac{\partial^4 f(0,\cdot)}{\partial x^4} + (d_5 l_5 - e_5)\frac{\partial^5 f(0,\cdot)}{\partial x^5}$$

$$+ (d_6 l_6 - e_6)\frac{\partial^6 f(0,\cdot)}{\partial x^6} + O(h^8). \tag{43}$$

Continuing similarly, the following dynamic weights and a fifth-order staggered boundary scheme are then obtained as follows:

$$-\frac{s_{0,1}}{h^2}f(0,\cdot) + \frac{s_{1,1}}{h^2}f(1,\cdot) - \frac{s_{2,1}}{h^2}f(2,\cdot) + \frac{s_{3,1}}{h^2}f(3,\cdot) - \frac{s_{4,1}}{h^2}f(4,\cdot) + f(5,\cdot) =$$

$$\frac{v_{1,1}}{h}\frac{\partial f(0,\cdot)}{\partial x} + v_{2,1}\frac{\partial^2 f(0,\cdot)}{\partial x^2} + v_{3,1}h\frac{\partial^3 f(0,\cdot)}{\partial x^3} + O(h^5), \tag{44}$$

where

$$s_{0,1} = i_4(i_3[i_2(i_1-1)-(j_1-1)]-[j_2(j_1-1)-(k_1-1)])$$

$$-(j_3[j_2(\gamma_2 j_1-\gamma_3)-(k_1-1)]-[k_2(k_1-1)-(l_1-1)]), \tag{45}$$

$$s_{1,1} = i_4 i_3 i_2 i_1, \qquad s_{2,1} i_4 i_3 i_2 + i_4 i_3 j_1 + i_4 j_2 j_1 + j_3 j_2 j_1, \tag{46}$$

$$s_{3,1} = i_4 i_3 + i_4 j_2 + i_4 k_1 + j_3 k_1 + j_3 j_2 + k_2 k_1, \qquad s_{4,1} = i_4 + j_3 + k_2 + l_1, \tag{47}$$

$$v_{1,1} = i_4(i_3[i_2(\gamma_1 i_1-\gamma_2)-(\gamma_2 j_1-\gamma_3)]-[j_2(\gamma_2 j_1-\gamma_3)-(\gamma_3 k_1-\gamma_4)])$$

$$-(j_3[j_2(\gamma_2 j_1-\gamma_3)-(\gamma_3 k_1-\gamma_4)]-[k_2(\gamma_3 k_1-\gamma_4)-(\gamma_4 l_1-\gamma_5)]), \tag{48}$$

$$v_{2,1} = \frac{1}{2!} i_4(i_3[i_2(\gamma_1^2 i_1-\gamma_2^2)-(\gamma_2^2 j_1-\gamma_3^2)]-[j_2(\gamma_2^2 j_1-\gamma_3^2)-(\gamma_3^2 k_1-\gamma_4^2)])$$

$$-\frac{1}{2!}(j_3[j_2(\gamma_2^2 j_1-\gamma_3^2)-(\gamma_3^2 k_1-\gamma_4^2)]-[k_2(\gamma_3^2 k_1-\gamma_4^2)-(\gamma_4^2 l_1-\gamma_5^2)]), \tag{49}$$

$$v_{3,1} = \frac{1}{3!} i_4(i_3[i_2(\gamma_1^3 i_1-\gamma_2^3)-(\gamma_2^3 j_1-\gamma_3^3)]-[j_2(\gamma_2^3 j_1-\gamma_3^3)-(\gamma_3^3 k_1-\gamma_4^3)])$$

$$-\frac{1}{3!}(j_3[j_2(\gamma_2^3 j_1-\gamma_3^3)-(\gamma_3^3 k_1-\gamma_4^3)]-[k_2(\gamma_3^3 k_1-\gamma_4^3)-(\gamma_4^3 l_1-\gamma_5^3)]), \tag{50}$$

Here,

$$i_2 = \frac{b_6 j_1 - c_6}{a_6 i_1 - b_6}, \qquad j_2 = \frac{c_6 k_1 - d_6}{b_6 j_1 - c_6}, \qquad l_2 = \frac{d_6 l_1 - e_6}{c_6 k_1 - d_6}, \tag{51}$$

$$i_3 = \frac{j_2(b_5 j_1 - c_5)-(c_5 k_1 - d_5)}{i_2(a_5 i_1 - b_5)-(b_5 j_1 - c_5)}, \qquad j_3 = \frac{k_2(c_5 k_1 - d_5)-(d_5 l_1 - e_5)}{j_2(b_5 j_1 - c_5)-(c_5 k_1 - d_5)}, \tag{52}$$

$$i_3 = \frac{j_3[j_2(b_4 j_1 - c_4)-(c_4 k_1 - d_4)]-[k_2(c_4 k_1 - d_4)-(d_4 l_1 - e_4)]}{i_3[i_2(a_4 i_1 - b_4)-(b_4 j_1 - c_4)]-[j_2(b_4 j_1 - c_4)-(c_4 k_1 - d_4)]}, \tag{53}$$

It can be seen that the truncation error is given as

$$R = C_{\gamma_i} h^8 + O(h^9), \tag{54}$$

where

$$C_{\gamma_i} = \frac{1}{8!} i_4(i_3[i_2(\gamma_1^8 i_1-\gamma_2^8)-(\gamma_2^8 j_1-\gamma_3^8)]-[j_2(\gamma_2^8 j_1-\gamma_3^8)-(\gamma_3^8 k_1-\gamma_4^8)])$$

$$-\frac{1}{8!}(j_3[j_2(\gamma_2^8 j_1-\gamma_3^8)-(\gamma_3^8 k_1-\gamma_4^8)]-[k_2(\gamma_3^8 k_1-\gamma_4^8)-(\gamma_4^8 l_1-\gamma_5^8)]). \tag{55}$$

Notice that the parameter on the right-hand side of (53) is independent of h. It is important to further mention that even though we have $O(h^8)$ convergence, it is up to a constant factor C_{γ_i} which is γ_i dependent. For a uniform scheme, this constant is fixed. However, for the present high-order staggered scheme and observing (38) and (51)-(53), it can easily be seen that C_{γ_i} can vary substantially based on the controlling and adjustable factors γ_1, γ_2. γ_3, γ_4, and γ_5 which represent the grid points distribution. The constant factor C_{γ_i}, depending on how small or large it is, can enable us to obtain a more or less accurate numerical solution with coarse

grids. However, asymptotically, the high convergence rate may depend on the smoothness of the function and the implemented high-order scheme. Finding an optimal grid point distribution that minimizes C_{γ_i} can substantially enable a much more accurate numerical solution with a large step size. This process could further be trained to be adaptive. We hope to investigate this phenomenon in our future work. Heuristically, a simple computation reveals the following parameters for C_{γ_i} based on the grid points distribution

$$C_{\gamma_i} = 0.77143, \quad \gamma_1 = 2, \quad \gamma_2 = 3, \quad \gamma_3 = 4, \quad \gamma_4 = 5, \quad \gamma_5 = 6; \tag{56}$$

$$C_{\gamma_i} = 1.78646, \quad \gamma_1 = 2, \quad \gamma_2 = 4, \quad \gamma_3 = 5, \quad \gamma_4 = 6, \quad \gamma_5 = 7; \tag{57}$$

$$C_{\gamma_i} = 95.23810, \quad \gamma_1 = 2, \quad \gamma_2 = 4, \quad \gamma_3 = 6, \quad \gamma_4 = 8, \quad \gamma_5 = 10. \tag{58}$$

From (56)-(58), it can easily be seen that the value of C_{γ_i} for grid points distribution (2,3,4,5,6) is the smallest. This gain can improve accuracy in a non-asymptotic scenario when the grid is coarse. We provide our further observation based on this positive indication in the numerical example.

Furthermore, we also observed that shifting away from the left boundary at least up to the first two grid points when implementing the Taylor series expansion for computing the optimal exercise boundary provides a more efficient result. Hence, we always select $\bar{x} \geq 2h$ and $\bar{x} \ll x_{\max}$. If we choose a uniform step size, we obtain the following uniform fifth-order boundary scheme as

$$\begin{aligned} 625f(\bar{x},\cdot) - \frac{625}{4}f(2\bar{x},\cdot) + \frac{1024}{27}f(3\bar{x},\cdot) - \frac{625}{64}f(4\bar{x},\cdot) + f(5\bar{x},\cdot) = \frac{874853}{1728}f(0,\cdot) \\ + \frac{60095}{144}\bar{x}\frac{\partial f(0,\cdot)}{\partial x} + \bar{x}^2\frac{3425}{24}\frac{\partial^2 f(0,\cdot)}{\partial x^2} + \bar{x}^3\frac{125}{6}\frac{\partial^3 f(0,\cdot)}{\partial x^3} + O(h^8). \end{aligned} \tag{59}$$

The motivation for implementing the present high order dynamic and staggered scheme is to enable us to select grid points very close to the left boundary point location in such a way that we still shift away from the left boundary at least up to the first two grid points when implementing the both the extrapolated and conventional Taylor series expansion. We may refer the reader to Figures 1 and 2.

To compute the optimal exercise boundary with precise accuracy using our high order staggered boundary scheme, we consider the square root transformation first presented in the work of Kim et al. [17] for solving American options with front-fixing. We further refer the reader to the work of Kim et al. [17, 18], Lee [19], and Nwankwo and Dai [25, 26, 27] on various implementations of this transformation for improving accuracy and recovering convergence rate when pricing American style options. The square root function with fixed free-boundary is presented as follows:

$$Q(x,t) = \sqrt{U(x,t) - E - s_f(t)}, \qquad \forall x. \tag{60}$$

Kim et al. [17] and Lee [19] analysed the characteristic of $Q(x,t)$ and showed that the function has a Lipschitz character and exhibits non-degeneracy and non-singularity near the optimal exercise boundary. It is well known that these degeneracy and singularity deteriorate the accuracy of American options. Furthermore, the authors proved in their work that sufficient large angle exists between the exercise region and continuation region such that

$$m_1 \leq \frac{\partial Q(0,t)}{\partial x} \leq m_2, \qquad m_1, m_2 > 0. \tag{61}$$

Here, we consider up to the third-order derivative (in space) of the function at the left boundary point with

$$Q(0,t)=0, \qquad \frac{\partial Q(0,t)}{\partial x}=\frac{rE}{\sigma}, \qquad \frac{\partial^2 Q(0,t)}{\partial x^2}=\frac{2\beta_t\sqrt{rE}}{3\sigma^3}, \tag{62}$$

$$\frac{\partial^3 Q(0,t)}{\partial x^3}=\frac{2\beta_t^2\sqrt{rE}}{3\sigma^5}+\frac{r\sqrt{rE}}{2\sigma^3}, \tag{63}$$

Substituting (62) and (63) for $\frac{\partial f(0,t)}{\partial x}$, $\frac{\partial^2 f(0,t)}{\partial x^2}$, and $\frac{\partial^3 f(0,t)}{\partial x^3}$ on the right-hand-side of (44), we obtain

$$-\frac{s_{0,1}}{h^2}f(0,\cdot)+\frac{s_{1,1}}{h^2}f(1,\cdot)-\frac{s_{2,1}}{h^2}f(2,\cdot)+\frac{s_{3,1}}{h^2}f(3,\cdot)-\frac{s_{4,1}}{h^2}f(4,\cdot)+f(5,\cdot)$$

$$=v_{1,1}\frac{rE}{\sigma h}+v_{2,1}\frac{2\beta_t\sqrt{rE}}{3\sigma^3}+v_{3,1}h\left(\frac{2\beta_t^2\sqrt{rE}}{3\sigma^5}+\frac{r\sqrt{rE}}{2\sigma^3}\right)+O(h^5), \tag{64}$$

The optimal exercise boundary is then computed as follows [17]:

$$\frac{ds_f(t)}{dt}=g_{h,t}s_f(t), \qquad g_{h,t}=\frac{\varpi-\sqrt{\varpi^2-4\alpha\kappa_{h,t}}}{2\alpha}; \tag{65}$$

where

$$\alpha=\frac{h^3\sqrt{rE}}{3\sigma^5 s_f^2(t)}v_{3,1}, \qquad \varpi=\frac{2h^2\sqrt{rE}}{3\sigma^3 s_f(t)}v_{2,1}+\frac{4h^3\sqrt{rE}}{3\sigma^5 s_f}v_{3,1}; \tag{66}$$

$$\kappa_{h,t}=-M_{5,1}+\frac{h\sqrt{rE}}{\sigma}v_{1,1}-\frac{h^2\left(r-\frac{\sigma^2}{2}\right)\sqrt{rE}}{3\sigma^3}v_{2,1}$$

$$+\frac{2h^3\left(r-\frac{\sigma^2}{2}\right)^2\sqrt{rE}}{3\sigma^5}v_{3,1}+\frac{h^3 r\sqrt{rE}}{2\sigma^3}v_{3,1}, \tag{67}$$

$$M_{5,1}=s_{1,1}Q(h_1,\cdot)-s_{2,1}Q(h_2,\cdot)+s_{3,1}Q(h_3,\cdot)-s_{4,1}Q(h_4,\cdot)+s_{5,1}Q(h_5,\cdot). \tag{68}$$

Furthermore, we can generate another high-order staggered boundary scheme with fewer stencils. To this end, following a similar approach as presented in (33)-(44), we obtain:

$$-\frac{s_{0,2}}{h^2}f(0,\cdot)+\frac{s_{1,2}}{h^2}f(1,\cdot)-\frac{s_{2,2}}{h^2}f(2,\cdot)+\frac{s_{3,2}}{h^2}f(3,\cdot)-\frac{s_{4,2}}{h^2}f(4,\cdot)+f(5,\cdot)=$$

$$\frac{v_{1,2}}{h}\frac{\partial f(0,\cdot)}{\partial x}+v_{2,2}\frac{\partial^2 f(0,\cdot)}{\partial x^2}+v_{3,1}\frac{\partial^3 f(0,\cdot)}{\partial x^3}+O(h^5), \tag{69}$$

where

$$i_5=\frac{b_6}{a_6}, \qquad j_5=\frac{c_6}{b_6}, \qquad k_5=\frac{d_6}{c_6}, \qquad l_5=\frac{e_6}{d_6}; \tag{70}$$

$$i_6=\frac{b_5 j_5-c_5}{a_5 i_5-b_5}, \qquad j_6=\frac{c_5 k_5-d_5}{b_5 j_5-c_5}, \qquad k_6=\frac{d_5 l_5-e_5}{c_5 k_5-d_5}; \tag{71}$$

$$i_7=\frac{j_6(b_4 j_5-c_4)-(c_4 k_5-d_4)}{i_6(a_4 i_5-b_4)-(b_4 j_5-c_4)}, \qquad j_7=\frac{k_6(c_4 k_5-d_4)-(d_4 l_5-e_4)}{j_6(b_4 j_5-c_4)-(c_4 k_5-d_4)}, \tag{72}$$

$$i_8 = \frac{j_7[j_6(b_3j_5 - c_3) - (c_3k_5 - d_3)] - [k_6(c_3k_5 - d_3) - (d_3l_5 - e_3)]}{i_7[i_6(a_3i_5 - b_3) - (b_3j_5 - c_3)] - [j_6(b_3j_5 - c_3) - (c_3k_5 - d_3)]}, \tag{73}$$

$$\begin{aligned} s_{0,2} =& i_8(i_7[i_6(i_5 - 1) - (j_5 - 1) - \\ & (k_5 - 1)]) - (j_7[j_6(j_5 - 1) - (k_5 - 1)] \end{aligned}$$

$$- (j_7[j_6(j_5 - 1) - (k_5 - 1)] - [k_6(k_5 - 1) - (l_5 - 1)]), \tag{74}$$

$$s_{1,2} = i_8i_7i_6i_5, \qquad s_{2,2} = i_8i_7i_6 + i_8i_7i_5 + i_7j_6j_5 + j_7j_6j_5, \tag{75}$$

$$s_{3,2} = i_8i_7 + i_8i_6 + i_8k_5 + j_7k_5 + j_7j_6 + +k_6k_5, \qquad s_{4,2} = i_8 + j_7 + k_6 + l_5, \tag{76}$$

$$\begin{aligned} v_{1,2} =& i_8(i_7[i_6(\gamma_1i_5 - \gamma_2) - (\gamma_2j_5 - \gamma_3) - \\ & (\gamma_3k_5 - \gamma_4)]) - (j_7[j_6(\gamma_2j_5 - \gamma_3) - (\gamma_3k_5 - \gamma_4)] \end{aligned}$$

$$- (j_7[j_6(\gamma_2j_5 - \gamma_3) - (\gamma_3k_5 - \gamma_4)] - [k_6(\gamma_3k_5 - \gamma_4) - (\gamma_4l_5 - \gamma_5)]), \tag{77}$$

$$\begin{aligned} v_{2,2} =& \frac{1}{2!}i_8(i_7[i_6(\gamma_1^2i_5 - \gamma_2^2) - (\gamma_2^2j_5 - \gamma_3^2) - \\ & (\gamma_3^2k_5 - \gamma_4^2)]) - (j_7[j_6(\gamma_2^2j_5 - \gamma_3^2) - (\gamma_3^2k_5 - \gamma_4^2)] \end{aligned}$$

$$- \frac{1}{2!}(j_7[j_6(\gamma_2^2j_5 - \gamma_3^2) - (\gamma_3^2k_5 - \gamma_4^2)] - [k_6(\gamma_3^2k_5 - \gamma_4^2) - (\gamma_4^2l_5 - \gamma_5^2)]). \tag{78}$$

Subtracting (44) from (69), we obtain the second staggered high-order boundary scheme

$$\begin{aligned} & -\frac{s_{0,1} - s_{0,2}}{h^2}f(0,\cdot) + \frac{s_{1,1} - s_{1,2}}{h^2}f(1,\cdot) - \frac{s_{2,1} - s_{2,2}}{h^2}f(2,\cdot) + \frac{s_{3,1} - s_{3,2}}{h^2}f(3,\cdot) \\ & - \frac{s_{4,1} - s_{4,2}}{h^2}f(4,\cdot) + f(5,\cdot) = \frac{v_{1,1} - v_{1,2}}{h}\frac{\partial f(0,\cdot)}{\partial x} + (v_{2,1} - v_{2,2})\frac{\partial^2 f(0,\cdot)}{\partial x^2} \end{aligned}$$

$$+ (v_{3,1} - v_{3,2})\frac{\partial^3 f(0,\cdot)}{\partial x^3} + O(h^5), \tag{79}$$

Substituting (62) into the right-hand side of (79)

$$\begin{aligned} & -\frac{s_{0,1} - s_{0,2}}{h^2}f(0,\cdot) + \frac{s_{1,1} - s_{1,2}}{h^2}f(1,\cdot) - \frac{s_{2,1} - s_{2,2}}{h^2}f(2,\cdot) + \frac{s_{3,1} - s_{3,2}}{h^2}f(3,\cdot) \\ & - \frac{s_{4,1} - s_{4,2}}{h^2}f(4,\cdot) + f(5,\cdot) = (v_{1,1} - v_{1,2})\frac{rE}{\sigma h} + (v_{2,1} - v_{2,2})\frac{2\beta_t\sqrt{rE}}{3\sigma^3} \end{aligned}$$

$$+ (v_{3,1} - v_{3,2})h\left(\frac{2\beta_t^2\sqrt{rE}}{3\sigma^5} + \frac{r\sqrt{rE}}{2\sigma^3}\right) + O(h^5), \tag{80}$$

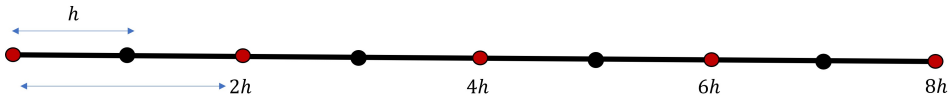

FIGURE 1. High order boundary scheme with uniform grid points $\bar{x} = 2h$. The grid points in red represent those involved in the computation of the optimal exercise boundary.

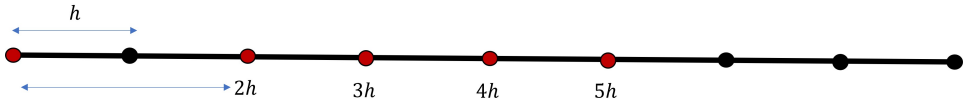

FIGURE 2. High order staggered boundary scheme with grid point distribution $(\gamma_1, \gamma_2, \gamma_3, \gamma_4) = (2, 3, 4, 5)$. The grid points in red represent those involved in the computation of the optimal exercise boundary.

It is important to mention that the present high-order staggered boundary schemes with 4 and 5 stencils can be used to generate arbitrary weights based on the selected grid point distribution. It gives us a control of the non-uniformity of our scheme and the choice of grid point by simply adjusting the parameter γ_1, γ_2, γ_3, γ_4, γ_5. This approach can further be extended to generate boundary schemes with lower-order accuracy when a low-order interior scheme is implemented.

2.3. Runge-Kutta 3(2) Bogacki and Shampine Adaptive Time-Stepping. Several Runge-Kutta embedded pairs have been proposed and implemented in works of literature [2, 3, 4, 5, 11, 12, 13, 16, 21, 25, 26, 27, 28, 30, 31, 32, 34, 36, 37]. Here, we consider 3(2) Bogacki-Shampine embedded pairs in [2] which are third-order accurate. The authors argued that it outperforms other existing third-order accurate methods with the second-order embedded method. Furthermore, efficient implementation of 5(4) embedded pairs for solving systems of diffusion-convective-reactive partial differential equations arising in the American options problem was described in the works of Nwankwo and Dai [25, 26, 27]. We further refer the reader to their works. Here, we slightly present some minor enhancements. The computational procedure for the implementation of the sixth-order compact scheme with 3(2) Bogacki-Shampine pairs is given as follows:

With slight abuse of notations, we let the two semi-discrete coupled systems of equations representing the asset option and delta sensitivity with the optimal exercise boundary be given as

$$\frac{\partial \mathbf{u}^n}{\partial t} = \mathbf{L}_u^n, \qquad \frac{\partial \mathbf{w}^n}{\partial t} = \mathbf{L}_w^n;$$

$$\mathbf{L}_u^n = \frac{\sigma^2}{2} B_5^{-1} \left(A_h \mathbf{u}^n + \mathbf{f}_{u,h}^n \right) + \beta^n \mathbf{w}^n - r\mathbf{u}^n,$$

$$\mathbf{L}_w^n = \frac{\sigma^2}{2} B_5^{-1} \left(A_h \mathbf{w}^n + \mathbf{f}_{w,h}^n \right) + \beta^n B_5^{-1} \left(A_h \mathbf{u}^n + \mathbf{f}_{u,h}^n \right) - r\mathbf{w}^n.$$

Ist computational stage:

$$\mathcal{L}_{s_f}^n = g_h^n s_f^n, \qquad \beta_n = \frac{\mathcal{L}_{s_f}^n}{s_f^n} + \nu, \qquad \nu = r - \frac{\sigma^2}{2};$$

$$\mathbf{L}_u^n = \frac{\sigma^2}{2} B_5^{-1}\left(A_h \mathbf{u}^n + \mathbf{f}_{u,h}^n\right) + \beta^n \mathbf{w}^n - r\mathbf{u}^n,$$

$$\mathbf{L}_w^n = \frac{\sigma^2}{2} B_5^{-1}\left(A_h \mathbf{w}^n + \mathbf{f}_{w,h}^n\right) + \beta^n B_5^{-1}\left(A_h \mathbf{u}^n + \mathbf{f}_{u,h}^n\right) - r\mathbf{w}^n,$$

$$s_f^{n+\frac{1}{4}} = s_f^n + \frac{1}{2}k\mathcal{L}_{s_f}^n, \qquad \mathbf{u}^{n+\frac{1}{4}} = \mathbf{u}^n + \frac{1}{2}k\mathbf{L}_u^n, \qquad \mathbf{w}^{n+\frac{1}{4}} = \mathbf{w}^n + \frac{1}{2}k\mathbf{L}_w^n.$$

2nd computational stage:

$$\mathcal{L}_{s_f^{n+\frac{1}{4}}}^n = g_h^{n+\frac{1}{4}} s_f^{n+\frac{1}{4}}, \qquad \beta^{n+\frac{1}{4}} = \frac{\mathcal{L}_{s_f}^{n+\frac{1}{4}}}{s_f^{n+\frac{1}{4}}} + \nu;$$

$$\mathbf{L}_u^{n+\frac{1}{4}} = \frac{\sigma^2}{2} B_5^{-1}\left(A_h \mathbf{u}^{n+\frac{1}{4}} + \mathbf{f}_{u,h}^{n+\frac{1}{4}}\right) + \beta^{n+\frac{1}{4}} \mathbf{w}^{n+\frac{1}{4}} - r\mathbf{u}^{n+\frac{1}{4}},$$

$$\mathbf{L}_w^{n+\frac{1}{4}} = \frac{\sigma^2}{2} B_5^{-1}\left(A_h \mathbf{w}^{n+\frac{1}{4}} + \mathbf{f}_{w,h}^{n+\frac{1}{4}}\right) + \beta^{n+\frac{1}{4}} B_5^{-1}\left(A_h \mathbf{u}^{n+\frac{1}{4}} + \mathbf{f}_{u,h}^{n+\frac{1}{4}}\right) - r\mathbf{w}^{n+\frac{1}{4}},$$

$$s_f^{n+\frac{2}{4}} = s_f^n + \frac{3}{4}k\mathcal{L}_{s_f}^n, \qquad \mathbf{u}^{n+\frac{2}{4}} = \mathbf{u}^n + \frac{3}{4}k\mathbf{L}_u^{n+\frac{1}{4}}, \qquad \mathbf{w}^{n+\frac{2}{4}} = \mathbf{w}^n + \frac{1}{2}k\mathbf{L}_w^{n+\frac{1}{4}},$$

3rd computational stage:

$$\mathcal{L}_{s_f^{n+\frac{2}{4}}}^n = g_h^{n+\frac{2}{4}} s_f^{n+\frac{2}{4}}, \qquad \beta^{n+\frac{2}{4}} = \frac{\mathcal{L}_{s_f}^{n+\frac{2}{4}}}{s_f^{n+\frac{2}{4}}} + \nu;$$

$$\mathbf{L}_u^{n+\frac{2}{4}} = \frac{\sigma^2}{2} B_5^{-1}\left(A_h \mathbf{u}^{n+\frac{2}{4}} + \mathbf{f}_{u,h}^{n+\frac{2}{4}}\right) + \beta^{n+\frac{2}{4}} \mathbf{w}^{n+\frac{2}{4}} - r\mathbf{u}^{n+\frac{2}{4}},$$

$$\mathbf{L}_w^{n+\frac{2}{4}} = \frac{\sigma^2}{2} B_5^{-1}\left(A_h \mathbf{w}^{n+\frac{2}{4}} + \mathbf{f}_{w,h}^{n+\frac{2}{4}}\right) + \beta^{n+\frac{2}{4}} B_5^{-1}\left(A_h \mathbf{u}^{n+\frac{2}{4}} + \mathbf{f}_{u,h}^{n+\frac{2}{4}}\right) - r\mathbf{w}^{n+\frac{2}{4}},$$

$$s_f^{n+\frac{3}{4}} = s_f^n + k\left(\frac{2}{9}\mathcal{L}_{s_f}^n + \frac{1}{3}\mathcal{L}_{s_f}^{n+\frac{1}{4}} + \frac{4}{9}\mathcal{L}_{s_f}^{n+\frac{2}{4}}\right).$$

$$\mathbf{u}^{n+\frac{3}{4}} = \mathbf{u}^n + k\left(\frac{2}{9}\mathbf{L}_u^n + \frac{1}{3}\mathbf{L}u^{n+\frac{1}{4}} + \frac{4}{9}\mathbf{L}_u^{n+\frac{2}{4}}\right).$$

$$\mathbf{w}^{n+\frac{3}{4}} = \mathbf{w}^n + k\left(\frac{2}{9}\mathbf{L}_w^n + \frac{1}{3}\mathbf{L}w^{n+\frac{1}{4}} + \frac{4}{9}\mathbf{L}_w^{n+\frac{2}{4}}\right),$$

4th computational stage:

$$\mathcal{L}_{s_f^{n+\frac{3}{4}}}^n = g_h^{n+\frac{3}{4}} s_f^{n+\frac{3}{4}}, \qquad \beta^{n+\frac{3}{4}} = \frac{\mathcal{L}_{s_f}^{n+\frac{3}{4}}}{s_f^{n+\frac{3}{4}}} + \nu;$$

$$\mathbf{L}_u^{n+\frac{3}{4}} = \frac{\sigma^2}{2} B_5^{-1}\left(A_h \mathbf{u}^{n+\frac{3}{4}} + \mathbf{f}_{u,h}^{n+\frac{3}{4}}\right) + \beta^{n+\frac{3}{4}} \mathbf{w}^{n+\frac{3}{4}} - r\mathbf{u}^{n+\frac{3}{4}},$$

$$\mathbf{L}_w^{n+\frac{3}{4}} = \frac{\sigma^2}{2} B_5^{-1}\left(A_h \mathbf{w}^{n+\frac{3}{4}} + \mathbf{f}_{w,h}^{n+\frac{3}{4}}\right) + \beta^{n+\frac{3}{4}} B_5^{-1}\left(A_h \mathbf{u}^{n+\frac{3}{4}} + \mathbf{f}_{u,h}^{n+\frac{3}{4}}\right) - r\mathbf{w}^{n+\frac{3}{4}},$$

$$s_f^{n+1} = s_f^{n+\frac{3}{4}}, \qquad \bar{s}_f^{n+1} = s_f^n + k\left(7\mathcal{L}_{s_f}^n + 6\mathcal{L}_{s_f}^{n+\frac{1}{4}} + 8\mathcal{L}_{s_f}^{n+\frac{2}{4}} + 3\mathcal{L}_{s_f}^{n+\frac{3}{4}}\right),$$

$$\mathbf{u}^{n+1} = \mathbf{u}^{n+\frac{3}{4}}, \qquad \bar{\mathbf{u}}^{n+1} = \mathbf{u}^n + k\left(7\mathbf{L}_u^n + 6\mathbf{L}u^{n+\frac{1}{4}} + 8\mathbf{L}_u^{n+\frac{2}{4}} + 3\mathbf{L}_u^{n+\frac{3}{4}}\right),$$

$$\mathbf{w}^{n+1} = \mathbf{w}^{n+\frac{3}{4}}, \qquad \bar{\mathbf{w}}^{n+1} = \mathbf{w}^n + k\left(7\mathbf{L}_w^n + 6\mathbf{L}w^{n+\frac{1}{4}} + 8\mathbf{L}_w^{n+\frac{2}{4}} + 3\mathbf{L}_w^{n+\frac{3}{4}}\right).$$

An error threshold is defined as follows:

$$(81)\quad e_u = ||\bar{\mathbf{u}}^{n+1} - \mathbf{u}^{n+1}||_\infty, \qquad e_w = ||\bar{\mathbf{w}}^{n+1} - \mathbf{w}^{n+1}||_\infty, \qquad e_{s_f} = |\bar{s}_f^{n+1} - s_f^{n+1}|,$$

such that we update the new time step at each time level based on the criterion below

$$k_{new} = \rho k_{old}\left(\frac{\varepsilon}{\max\{e_u, e_w, e_{s_f}\}}\right)^{\frac{1}{2}}, \qquad \max\{e_u, e_w, e_{s_f}\} < \varepsilon; \tag{82}$$

$$k_{new} = \rho k_{old}\left(\frac{\varepsilon}{\max\{e_u, e_w, e_{s_f}\}}\right)^{\frac{1}{3}}, \qquad \max\{e_u, e_w, e_{s_f}\} \geq \varepsilon. \tag{83}$$

Here, ε is a given tolerance and $0 < \rho < 1$. Moreover, k_{new} represent the optimal time step if $\max\{e_u, e_w, e_{s_f}\} < \varepsilon$ and as such, $k_{new} = k$ and the obtained numerical solutions of the optimal exercise boundary, asset option, and delta sensitivity are accepted. If $\max\{e_u, e_w, e_{s_f}\} \geq \varepsilon$, we obtain a new time step based on (83) and go back to stage 1. The process continues till if $\max\{e_u, e_w, e_{s_f}\} < \varepsilon$ is achieved. In the numerical example section, we will vary ρ and observe its effect on the computational time and accuracy of our numerical approximations.

2.4. Second-order derivative of the optimal exercise boundary. In this study, we are more interested to investigate the profiles of the derivatives of the optimal exercise boundary after improving it using the high-order analytical approximation as presented in Subsection 2.2. We consider up to the second-order derivative of the optimal exercise boundary. For the second-order derivative of the optimal exercise boundary, we need to consider some extra derivations as follows:

$$U(x,t) = Q^2(x,t) + E - e^x s_f(t), \tag{84}$$

$$U_{x^3}(0,t) = -\frac{4\left(r - \frac{\sigma^2}{2}\right)rE}{\sigma^4} - \frac{4rE}{\sigma^4 s_f(t)}\frac{ds_f(t)}{dt} - s_f(t), \tag{85}$$

$$U_{x^3t}(0,t) = -\frac{4rE}{\sigma^4 s_f(t)}\frac{d^2 s_f(t)}{dt^2} + \frac{4rE}{\sigma^4 s_f^2(t)}\left(\frac{ds_f(t)}{dt}\right)^2 - \frac{ds_f(t)}{dt}, \tag{86}$$

$$U_{x^4}(0,t) = \frac{8\beta^2 rE}{\sigma^6} + \frac{4r^2E}{\sigma^4} - s_f(t), \tag{87}$$

$$U_{x^5}(0,t) = -\frac{80\beta^3 rE}{9\sigma^8} + \frac{4r^2E}{\sigma^4} - \frac{80\beta^3 rE}{9\sigma^8} + \frac{10\sqrt{rE}}{\sigma}U_{x^4}(0,t) - s_f(t). \tag{88}$$

Differentiating the transformed American options model in (7) thrice and substituting (85)-(88), we obtain

$$\begin{aligned} &-\frac{4rE}{\sigma^4 s_f(t)}\frac{ds_f^2(t)}{dt^2} + \frac{4rE}{\sigma^4 s_f^2(t)}\left(\frac{ds_f(t)}{dt}\right)^2 - \frac{ds_f(t)}{dt} \\ &- \frac{\sigma^2}{2}\left(-\frac{80\beta^3 rE}{9\sigma^8} + \frac{4r^2E}{\sigma^4} - \frac{80\beta^3 rE}{9\sigma^8} + \frac{10\sqrt{rE}}{\sigma}U_{x^4}(0,t) - s_f(t)\right) \\ &- \beta_t\left(\frac{8\beta^2 rE}{\sigma^6} + \frac{4r^2E}{\sigma^4} - s_f(t)\right) + r\left(-\frac{4r\beta_t}{\sigma^4}\right) = 0. \end{aligned} \tag{89}$$

Solving for $Q_{x^4}(0,t)$, we obtain

(90)
$$Q_{x^4}(0,t) = -\frac{4\sqrt{rE}}{5\sigma^5 s_f(t)}\frac{ds_f^2(t)}{dt^2} + \frac{4\sqrt{rE}}{5\sigma^5 s_f^2(t)}\left(\frac{ds_f(t)}{dt}\right)^2 - \frac{32\beta_t^3\sqrt{rE}}{45\sigma^7} - \frac{14\beta_t r\sqrt{rE}}{15\sigma^5}.$$

Furthermore, as mentioned earlier, $\bar{x} \ll x$ and if we chose $\bar{x} = 2h$ and ignore $Q(0,\cdot) = 0$ another high-order analytical approximation for approximating the second-order derivative of the optimal exercise boundary is introduced as follows:

$$1024Q(\bar{x},\cdot) - 96Q(2\bar{x},\cdot) + \frac{1024}{81}Q(\bar{3}x,\cdot) - Q(4\bar{x},\cdot) = \frac{23380}{27}\bar{x}Q_x(0,\cdot)$$

(91)
$$+ \frac{3320}{9}\bar{x}^2 Q_{x^2}(0,\cdot) + \frac{800}{9}\bar{x}^3 Q_{x^3}(0,\cdot) + \frac{32}{3}\bar{x}^4 Q_{x^4}(0,\cdot) + O(h^8).$$

We then compute the second-order derivative of the optimal exercise boundary as follows:

$$\frac{d^2 s_f(t)}{dt^2} = -\varrho(t)\left(M_{4,h} - \frac{23380\bar{x}\sqrt{rE}}{27\sigma}\right)$$

$$- \varrho(t)\left[\frac{6640\bar{x}^2\beta_t\sqrt{rE}}{27\sigma^3} - \frac{800\bar{x}^3}{9}\left(\frac{2\beta_t^2\sqrt{rE}}{3\sigma^5} + \frac{r\sqrt{(rE}}{2\sigma^3}\right)\right]$$

(92)
$$- \frac{32\varrho(t)}{3}\left[\frac{4\bar{x}^4\sqrt{rE}}{5\sigma^5 s_f^2(t)}\left(\frac{ds_f(t)}{dt}\right)^2 - \frac{32\bar{x}^4\beta_t^3\sqrt{rE}}{45\sigma^7} - \frac{14\bar{x}^4\beta_t r\sqrt{rE}}{15\sigma^5}\right].$$

Here,

(93)
$$\varrho(t) = \frac{5\sigma^5 s_f(t)}{4\sqrt{rE}}, \qquad M_{4,h} = 1024Q(\bar{x},\cdot) - 96Q(2\bar{x},\cdot) + \frac{1024}{81}Q(\bar{3}x,\cdot) - Q(4\bar{x},\cdot).$$

Because the equations for computing the first and second-order derivatives of the optimal exercise boundary do not directly involve time discretization, we can easily compute them using the numerical solutions of the asset option at the $nth-$time level based on (64) or (80) and (92).

3. Numerical Examples and Discussion

In this section, we consider three cases to verify and validate the performance of our present method with respect to computational cost, numerical accuracy, and recovering numerical convergence rate. To this end, we consider the following cases with short, medium, and a long time to maturity:

(94)
$$E = 100, \qquad r = 0.05, \qquad \sigma = 0.2, \qquad T = 0.5, 3.0;$$

(95)
$$E = 100, \qquad r = 0.1, \qquad \sigma = 0.3, \qquad T = 1.0;$$

(96)
$$E = 100, \qquad r = 0.08, \qquad \sigma = 0.2, \qquad T = 3.0.$$

Here, we use varying large tolerances and step sizes and adapt our time stepping to be optimal at each time level based on the given tolerance and step size. Our code is written in MATLAB R2022b with a laptop speed of 1.7GHz. For convenience, we label our method as follows:

- Sixth-order compact scheme with fifth-order near-boundary scheme and 5-stencil fifth-order staggered boundary scheme-CC-55 (γ_1, γ_2, γ_3, γ_4, γ_5).
- Sixth-order compact scheme with fifth-order near-boundary scheme and 4-stencil fifth-order staggered boundary scheme-CC-54 (γ_1, γ_2, γ_3, γ_4).

3.1. Convergence Rate Result. We computed the convergence rate of our numerical scheme using the case in (94) and verify how well it agrees with its theoretical counterpart. Because our adaptive scheme is third-order accurate, we computed the convergence rate of our numerical scheme using SSPRK3 which has strong stability property [14, 29] and is third-order accurate. We computed the convergence rates of the asset option, delta sensitivity, optimal exercise boundary, and the derivative of the optimal exercise boundary with $k = 10^{-6}$. It is worth mentioning that to the best of our knowledge, that this is the first time the convergence rate of the first derivative of the optimal exercise boundary is accounted for in literature. The results were displayed in Tables 1-2.

From Tables 1-2, one can easily see that the obtained convergence rate is in very good agreement with the implemented scheme as the step size decreases. It is better than the one we obtained in our previous work [25, 26, 27] where we implemented a fourth-order compact scheme. Also, a very high convergence rate was obtained for the first-order derivative of the optimal exercise boundary. This is because we computed the latter with the high-order analytical approximation. Furthermore, in most cases, the error decreases a bit faster in grid points distributions (γ_1, γ_2, γ_3, γ_4) $= (2, 3, 4, 5)$ and (γ_1, γ_2, γ_3, γ_4, γ_5) $= (2, 3, 4, 5, 6)$ when compared with (γ_1, γ_2, γ_3, γ_4) $= (2, 4, 5, 6)$, (γ_1, γ_2, γ_3, γ_4, γ_5) $= (2, 4, 5, 6, 7)$,(γ_1, γ_2, γ_3, γ_4) $= (2, 4, 6, 8)$, and (γ_1, γ_2, γ_3, γ_4, γ_5) $= (2, 4, 6, 8, 10)$.

3.2. Numerical solution and comparison. We computed the numerical solution of the asset option for the case in (96). The benchmark value was obtained from the work of Cox et al. [10]. The results were displayed in Table 3. We also computed the numerical solutions of the optimal exercise boundary and its derivatives with varying distributions of grid points. The numerical solutions were listed in Table 8 for the case in (95). We displayed the plot profiles of the optimal exercise boundary with its first and second-order derivatives in Figure 3 for the case in (96).

TABLE 1. Maximum error and convergence rates in space with CC-55.

h	Max. error	Convergence rate	Max. error	Convergence rate
(2,3,4,5,6)				
	Options value		Delta sensitivity	
0.1	–	–	–	–
0.05	6.080×10^{-1}	–	4.683×10^{0}	–
0.025	4.807×10^{-2}	3.085	7.148×10^{-1}	2.804
0.0125	8.726×10^{-4}	6.359	1.177×10^{-2}	7.263
0.00625	2.643×10^{-5}	5.045	1.882×10^{-4}	4.608
Average CR		4.829		4.891
	Opt. exer. boundary		Opt. exer. boundary derivative	
0.1	–	–	–	–
0.05	6.080×10^{-1}	–	6.509×10^{0}	–
0.025	4.807×10^{-2}	3.661	9.320×10^{-1}	2.804
0.0125	2.879×10^{-4}	7.384	6.066×10^{-3}	7.263
0.00625	1.502×10^{-5}	4.261	2.487×10^{-4}	4.608
Average CR		5.012		4.891
(2,4,5,6,7)				
	Options value		Delta sensitivity	
0.1	–	–	–	–
0.05	1.322×10^{0}	–	7.833×10^{1}	–
0.025	6.621×10^{-2}	4.330	7.034×10^{-1}	3.477
0.0125	2.117×10^{-3}	4.967	1.623×10^{-2}	5.437
0.00625	9.130×10^{-5}	4.536	5.578×10^{-4}	4.863
Average CR		4.611		4.592
	Opt. exer. boundary		Opt. exer. boundary derivative	
0.1	–	–	–	–
0.05	1.919×10^{0}	–	1.1047×10^{1}	–
0.025	4.854×10^{-2}	5.118	7.723×10^{-1}	3.761
0.0125	2.945×10^{-3}	4.456	5.129×10^{-3}	7.234
0.00625	1.327×10^{-4}	4.363	8.326×10^{-5}	5.945
Average CR		4.646		5.647
(2,4,6,8,10)				
	Options value		Delta sensitivity	
0.1	–	–	–	–
0.05	1.919×10^{0}	–	1.041×10^{1}	–
0.025	7.847×10^{-2}	4.612	8.004×10^{-1}	3.700
0.0125	3.241×10^{-3}	4.598	2.363×10^{-3}	5.081
0.00625	1.407×10^{-4}	4.525	8.436×10^{-4}	4.808
Average CR		4.578		4.529
	Opt. exer. boundary		Opt. exer. boundary derivative	
0.1	–	–	–	–
0.05	1.919×10^{0}	–	1.183×10^{1}	–
0.025	4.854×10^{-2}	5.304	6.956×10^{-1}	4.088
0.0125	2.945×10^{-3}	4.043	1.302×10^{-2}	5.739
0.00625	1.327×10^{-4}	4.472	2.758×10^{-4}	5.561
Average CR		4.606		5.620

TABLE 2. Maximum error and convergence rates in space with CC-54.

h	Max. error	Convergence rate	Max. error	Convergence rate
(2,3,4,5)				
	Options value		Delta sensitivity	
0.1	–	–	–	–
0.05	1.111×10^{0}	–	6.890×10^{1}	–
0.025	7.607×10^{-2}	3.868	7.542×10^{-1}	3.192
0.0125	1.682×10^{-2}	5.499	1.177×10^{-2}	5.824
0.00625	6.193×10^{-5}	4.764	1.882×10^{-4}	5.059
Average CR		4.710		4.692
	Opt. exer. boundary		Opt. exer. boundary derivative	
0.1	–	–	–	–
0.05	1.111×10^{0}	–	9.188×10^{0}	–
0.025	5.407×10^{-2}	4.461	8.443×10^{-1}	3.444
0.0125	1.245×10^{-3}	5.341	9.840×10^{-2}	9.796
0.00625	5.416×10^{-5}	4.523	8.988×10^{-4}	3.448
Average CR		4.775		5.562
(2,4,5,6)				
	Options value		Delta sensitivity	
0.1	–	–	–	–
0.05	1.962×10^{0}	–	1.061×10^{1}	–
0.025	7.814×10^{-2}	4.650	8.087×10^{-1}	3.713
0.0125	3.567×10^{-3}	4.453	2.569×10^{-2}	4.976
0.00625	1.495×10^{-4}	4.577	8.988×10^{-4}	4.837
Average CR		4.578		4.529
	Opt. exer. boundary		Opt. exer. boundary derivative	
0.1	–	–	–	–
0.05	1.962×10^{0}	–	1.167×10^{1}	–
0.025	4.747×10^{-2}	5.369	8.213×10^{-1}	3.829
0.0125	3.291×10^{-3}	3.851	1.635×10^{-2}	5.650
0.00625	1.408×10^{-4}	4.547	2.938×10^{-4}	5.799
Average CR		4.589		5.093
(2,4,6,8)				
	Options value		Delta sensitivity	
0.1	–	–	–	–
0.05	1.919×10^{0}	–	1.041×10^{1}	–
0.025	7.847×10^{-2}	4.876	8.004×10^{-1}	3.852
0.0125	3.241×10^{-3}	4.068	2.363×10^{-3}	4.678
0.00625	1.407×10^{-4}	4.585	8.436×10^{-4}	4.805
Average CR		4.510		4.205
	Opt. exer. boundary		Opt. exer. boundary derivative	
0.1	–	–	–	–
0.05	2.389×10^{0}	–	1.192×10^{1}	–
0.025	4.758×10^{-2}	5.650	9.817×10^{-1}	3.602
0.0125	4.596×10^{-3}	3.372	2.603×10^{-2}	5.237
0.00625	1.915×10^{-4}	4.585	5.015×10^{-4}	5.698
Average CR		4.535		4.846

TABLE 3. Comparison of the asset option for (96) using $\varepsilon = 10^{-4}$.

S	Benchmark value [10]		
100	6.9320		
110	4.1550		
	$(\gamma_1,\gamma_2,\gamma_3,\gamma_4) = (2,3,4,5)$		
	$h = 0.06$	$h = 0.03$	$h = 0.01$
100	6.9316	6.9323	6.9322
110	4.1551	4.1552	4.1550
	$(\gamma_1,\gamma_2,\gamma_3,\gamma_4) = (2,4,6,8)$		
100	6.9310	6.9324	6.9322
110	4.1543	4.1553	4.1550
	$(\gamma_1,\gamma_2,\gamma_3,\gamma_4) = (3,4,5,6)$		
	$h = 0.06$	$h = 0.03$	$h = 0.01$
100	6.9294	6.9325	6.9322
110	4.1524	4.1553	4.1550
	$(\gamma_1,\gamma_2,\gamma_3,\gamma_4) = (2,4,6,8)$		
100	6.9212	6.9326	6.9322
110	4.1427	4.1554	4.1550

TABLE 4. Comparison of the optimal exercise boundary and its derivatives for (95) using CC-54 and $\varepsilon = 10^{-4}$.

$(\gamma_1,\gamma_2,\gamma_3,\gamma_4) = (2,3,4,5)$			
h	76.16	6.9320	
$s_f(t)$	76.16	76.16	76.16
$s_f'(t)$	-4.59	-4.52	-4.51
$s_f''(t)$	61.53	30.65	10.20
	$(\gamma_1,\gamma_2,\gamma_3,\gamma_4) = (2,4,6,8)$		
$s_f(t)$	76.15	76.16	76.16
$s_f'(t)$	-4.63	-4.54	-4.51
$s_f''(t)$	96.75	48.11	15.11
	$(\gamma_1,\gamma_2,\gamma_3,\gamma_4) = (3,4,5,6)$		
$s_f(t)$	76.15	76.16	76.16
$s_f'(t)$	-4.68	-4.52	-4.51
$s_f''(t)$	58.90	29.28	9.74
	$(\gamma_1,\gamma_2,\gamma_3,\gamma_4) = (3,5,7,9)$		
	$h = 0.06$	$h = 0.03$	$h = 0.01$
$s_f(t)$	76.14	76.16	76.16
$s_f'(t)$	-4.47	-4.51	-4.51
$s_f''(t)$	93.65	46.74	15.53
	$(\gamma_1,\gamma_2,\gamma_3,\gamma_4) = (3,6,9,12)$		
$s_f(t)$	76.12	76.16	76.16
$s_f'(t)$	-4.48	-4.52	-4.51
$s_f''(t)$	128.63	64.25	21.33

TABLE 5. CPU time(s) and options price value for SSPRK3 using (96), $h = 0.02$, $\rho = 0.9$, CC-54, and $(\gamma_1, \gamma_2, \gamma_3, \gamma_4) = (2, 4, 6, 8)$. True value for $S = 90$ is 11.6976.

CPU time(s)		
$k = 4.0 \times 10^{-3}$	$k = 8.0 \times 10^{-4}$	$k = 4.0 \times 10^{-4}$
17	43	85
$S = 90$		
11.6967	11.6976	11.6976

TABLE 6. CPU time(s) and options price value for 3(2) Bogacki-Shampine pairs using (96), $h = 0.02$, $\rho = 0.9$, CC-54, and $(\gamma_1, \gamma_2, \gamma_3, \gamma_4) = (2, 4, 6, 8)$. True value for $S = 90$ is 11.6976.

$\varepsilon = 10^{-2}$				
CPU time(s)	$S = 90$	min . k	ave. k	max . k
11	11.6976	4.9×10^{-4}	7.1×10^{-3}	1.6×10^{-2}

TABLE 7. Comparing total CPU time(s) and options price value with 3(2) Bogacki-Shampine pairs using (96), $h = 0.02$, $\varepsilon = 10^{-2}$, CC-54, and $(\gamma_1, \gamma_2, \gamma_3, \gamma_4) = (2, 4, 6, 8)$. True value for $S = 90$ is 11.6976.

ρ	CPU time(s)	$S = 90$
0.20	8	11.6976
0.30	7	11.6976
0.40	10	11.6976
0.50	12	11.6976
0.55	11	11.6976
0.60	10	11.6976
0.65	11	11.6976
0.70	12	11.6976
0.75	12	11.6976
0.80	11	11.6976
0.85	12	11.6976

We observed from Tables 3 and 4 that the obtained results are very close to the benchmark value with very coarse grids. Furthermore, when the grid is very coarse, we observed that the numerical solution from the grid points distribution $(\gamma_1, \gamma_2, \gamma_3, \gamma_4)$ =(2,3,4,5) is the most accurate when compared with the solution obtained from $(\gamma_1, \gamma_2, \gamma_3, \gamma_4)$ =(2,4,6,8) ,(3,4,5,6), and (3,6,9,12) using the most coarse grid. Furthermore, In Table 4, it is important to observe how the numerical solution of the optimal exercise boundary and its derivatives behave based on the grid point distribution using the high-order staggered boundary scheme we presented in this work. For instance, the numerical solution using $(\gamma_1, \gamma_2, \gamma_3, \gamma_4)$ =(2,3,4,5) is almost the same as the one obtained from $(\gamma_1, \gamma_2, \gamma_3, \gamma_4)$ =(3,4,5,6). Also, the numerical solution obtained with grid points distribution $(\gamma_1, \gamma_2, \gamma_3, \gamma_4)$ =(2,4,6,8) is like the one obtained from $(\gamma_1, \gamma_2, \gamma_3, \gamma_4)$ =(3,5,7,9). As we have already mentioned, when the number of stencils increases, the high-order staggered boundary

schemes leverage the position to keep away from the left boundary as much as possible and still use grid points very close to the latter for computing the boundary values and the optimal exercise boundary. Hence, they enhance the accuracy of the numerical approximations of the optimal exercise boundary, asset option, and their derivatives.

TABLE 8. Comparison of the American put option price with some of the existing methods based on front-fixing technique.

S	WK [38]	FF [9]	H-FF [29]
		$h = 0.001$	$h = 0.008$
80	20.2825	20.2799	20.2806
90	13.3117	13.3077	13.3079
100	8.7135	8.7107	8.7105
110	5.6867	5.6695	5.6823
120	3.7001	3.6863	3.6961
$(\gamma_1, \gamma_2, \gamma_3, \gamma_4) = (2,4,6,8,10)$			
	$h = 0.05$	$h = 0.025$	$h = 0.01$
80	20.2940	20.2863	20.2820
90	13.3091	13.3078	13.3077
100	8.7128	8.7108	8.7107
110	5.6848	5.6827	5.6826
120	3.6986	3.6966	3.6964
$(\gamma_1, \gamma_2, \gamma_3, \gamma_4, \gamma_5) = (2,3,4,5,6)$			
	$h = 0.05$	$h = 0.025$	$h = 0.01$
80	20.2938	20.2863	20.2820
90	13.3083	13.3077	13.3077
100	8.7118	8.7107	8.7107
110	5.6838	5.6827	5.6826
120	3.6976	3.6965	3.6964

For instance, in our previous work [27] where we implemented a fourth-order compact finite difference scheme and fifth-order RK-Dormand and Prince embedded pairs [11] (which is one of 5(4) Runge-Kutta pairs that provides more accurate results), we obtained $s_f(t) = 76.17$ when $h = 0.06$. However, as shown in Table 4 with the grid point distribution $(\gamma_1, \gamma_2, \gamma_3, \gamma_4)$ =(2,3,4,5), we obtained exactly $s_f(t) = 76.17$ when $h = 0.06$. This shows that our sixth order scheme with the grid point distribution $(\gamma_1, \gamma_2, \gamma_3, \gamma_4)$ =(2,3,4,5) provides more accurate numerical solutions. In general, our numerical scheme yields highly accurate numerical approximations of the boundary values, asset option, and delta sensitivity with very coarse grids and large tolerance up to $\varepsilon = 10^{-2}$.

We also compared the total CPU time(s) and numerical accuracy between the SSPRK3 scheme and 3(2) Bogacki-Shampine pairs with varying large tolerances. Furthermore, we compared the total CPU time(s) and the accuracy of our numerical approximation with 3(2) Bogacki-Shampine pairs and varying ρ. The results were listed in Tables 5-7. For the computational time, when $h = 0.02$ and $\rho = 0.9$ we observed from Tables 5 and 6 that 3(2) Bogacki-Shampine embedded pairs is more than four times faster than SSPRK3 in achieving the same numerical accuracy. It implies that we can achieve greater accuracy with fast computation, very coarse grids, and large tolerance using 3(2) RK-Bogacki-Shampine pairs.

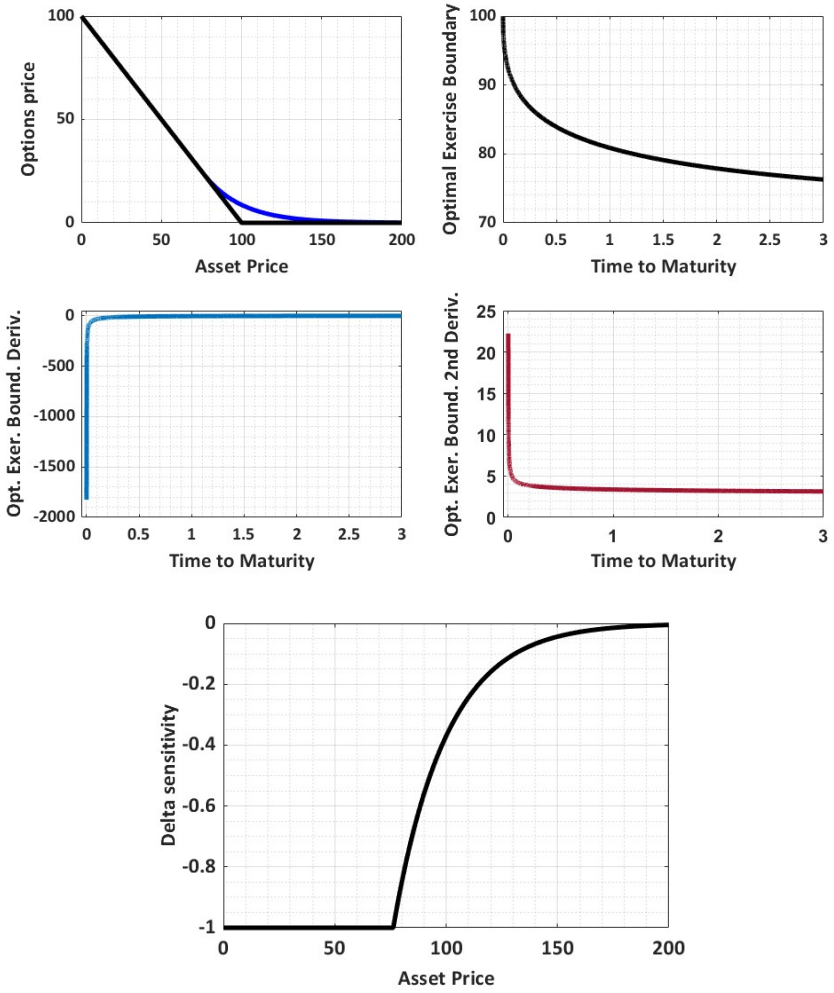

FIGURE 3. Profile of the option value, delta sensitivity, optimal exercise boundary, and the derivatives of the optimal exercise boundary with a long time to maturity (96), CC-54, $h = 0.0125$, $\rho = 0.3$, $\varepsilon = 10^{-6}$, and $(\gamma_1, \gamma_2, \gamma_3, \gamma_4) = (2,4,6,8)$.

Furthermore, in Table 7 using $h = 0.02$, it can be easily seen that when ρ is varied and for $\rho = 0.3$, we obtained the smallest total CPU total time of 7.0 seconds which is more than six times faster than SSPRK3 with the same accuracy. It is worth mentioning that we could further enhance our numerical result using higher-order embedded pairs. However, in this work, we focus on lower-order pairs which involve fewer functions evaluation.

For further comparison, we investigated the performance of our proposed method as compared with the results obtained from the existing methods that implemented front-fixing techniques which include the method work of Wu and Kwok [38], Company et al. [9], and Sari and Gulen [29]. Here, we considered the parameter in (94) for $T = 3.0$. The obtained result for this experiment was presented in Table 6.

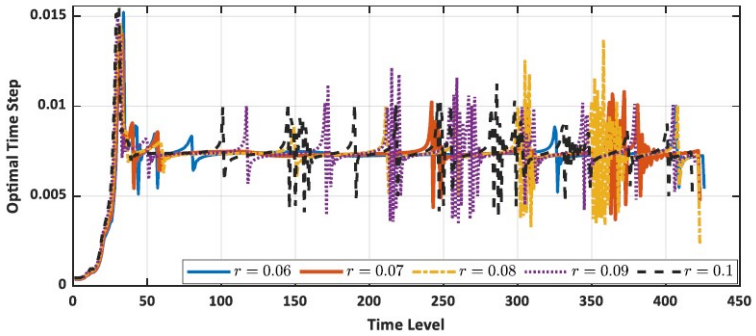

FIGURE 4. Profile of the optimal time step for each time level with CC-54, $h = 0.02$, $\varepsilon = 10^{-2}$, $(\gamma_1, \gamma_2, \gamma_3, \gamma_4) = (2,3,4,5)$ and 3(2) RK-Bogacki and Shampine embedded pairs. Here, $K = 100$, $\sigma = 0.2$, and $\sigma = 0.06, 0.07, 0.08, 0.09, 0.1$.

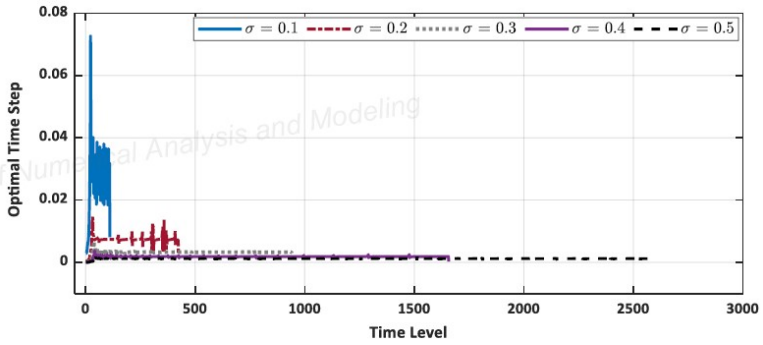

FIGURE 5. Profile of the optimal time step for each time level with CC-54, $h = 0.02$, $\varepsilon = 10^{-2}$, $(\gamma_1, \gamma_2, \gamma_3, \gamma_4) = (2,3,4,5)$ and 3(2) RK-Bogacki and Shampine embedded pairs. Here, $K = 100$, $r = 0.08$, and $\sigma = 0.1, 0.2, 0.3, 0.4, 0.5$.

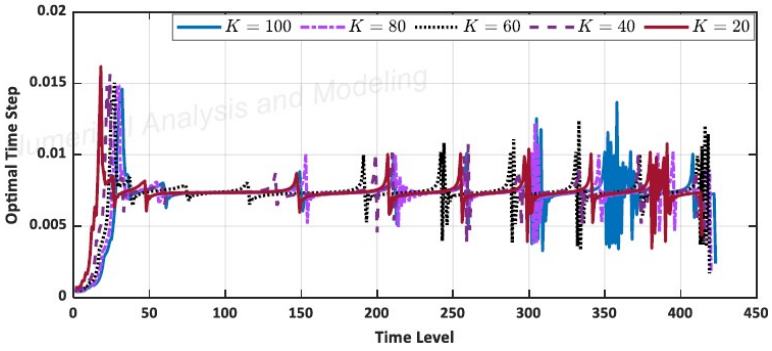

FIGURE 6. Profile of the optimal time step for each time level with CC-54, $h = 0.02$, $\varepsilon = 10^{-2}$, $(\gamma_1, \gamma_2, \gamma_3, \gamma_4) = (2,3,4,5)$ and 3(2) RK-Bogacki and Shampine embedded pairs. Here, $\sigma = 0.2$, $r = 0.08$, and $K = 100, 80, 60, 40, 20$.

We observed that with a reasonable coarse grid, our results are in close agreement with those obtained from existing methods.

Furthermore, we observe from Figure 3 that the numerical solutions of the first and second-order derivatives of the optimal exercise boundary are very smooth. It can easily be seen that $s_f''(t) > 0$ for all $t > 0$. Please see the work of Chen and Chadam [6, 7] and Chen et al. [8] based on the convexity of the optimal exercise boundary. Reflecting on the high convergence rate we obtained from the first-order derivative of the optimal exercise boundary, we can argue that our method is very efficient in approximating the optimal exercise boundary and its derivatives. It remains to be seen the importance of the first and second-order derivatives of the optimal exercise boundary in the pricing and hedging options.

Figures 4-6 show the plot profiles of the optimal time step for each time level. We would like to observe the sensitivities of the optimal time step for each time level with respect to the interest rate, volatility, and the strike price. This is because the option value and its numerical approximation strongly depend on these parameters. By formulating how we select the time step adaptively for each time level, we are interested in how the optimal time step for each time level changes across these important parameters when the latter is varied.

We observed from Figures 4-6 that the optimal time step selection is almost independent of the varying strike prices and interest rates but strongly dependent on the varying volatilities. If the other parameters are fixed as shown in Figure 5, a decrease in volatility value results in large time step selection for each time level and vice versa. Without the implementation of adaptive time stepping, likely, the stability of our numerical scheme may strongly depend on the volatility parameter. Like other RK-embedded pairs we have implemented in our previous works, one can easily observe in Figures 4-6 that a very small time step is required at the payoff and its neighbourhood for any set of parameters chosen. This is one of the well-known features of the Runge-Kutta adaptive time integration methods that allow the selection of small or large time steps in regions where there is high variation, oscillation, and/or discontinuity or sufficient smoothness, respectively. It is much expected because of the observable irregularity in this pricing model which occurs at the payoff.

4. Conclusion

We have developed a numerical method for pricing American options with optimal exercise boundary. In details, we employ a logarithmic Landau transformation to front-fix the computational free boundary at $x = 0$. However, a discontinuous coefficient that involves the derivative of the optimal exercise boundary is introduced in the convective term, which could deteriorate the accuracy of the American options. To overcome this challenge, we remove the convective term by introducing the delta sensitivity to obtain a new two-equation model coupling the option value and the delta sensitivity, as well as the optimal exercise boundary. We then employ a standard sixth-order compact finite difference scheme for both equations in the interior grid points and develop a novel fifth order staggered boundary scheme to incorporate the compact scheme. The optimal exercise boundary and other boundary values are approximated using a high-order analytical approximation that is obtained from the staggered boundary scheme. As such, a stable sixth-order compact finite difference scheme coupled with a fifth-order staggered boundary scheme and the Runge-Kutta adaptive time stepping based on 3(2) Bogacki-Shampine pairs

is obtained for pricing the American options. The precise values of the optimal exercise boundary, its derivatives, and the asset options and the delta sensitivity can be obtained with a rather coarse grid. Numerical results show that the expected convergence rate is obtained, and the present scheme is very fast in computation and give highly accurate solutions with very coarse grids.

Acknowledgments

The author thanks the Editors and anonymous reviewers for their valuable comments and suggestions which enhance the quality of our manuscript. The first author is funded in part by an NSERC Discovery Grant.

Conflict of interest

The authors declare that they have no conflict of interest.

CRediT authorship contribution statement

Nwankwo Chinonso: Conceptualization, Methodology, Software, Data curation, Formal analysis, Writing -original draft, Visualization, Investigation, Resources, Validation.: **Weizhong Dai**: Conceptualization, Supervision, Writing - review & editing, Project administration.

References

[1] Ballestra, L. V., Fast and Accurate Calculation of American Option Prices, Decisions in Economics and Finance, 41 (2018), 399-426.
[2] Bogacki, P. and Shampine, L. F., A 3(2) Pair of Runge-Kutta Formulas, Applied Mathematics Letter, 2 (1989), 321-325.
[3] Bogacki, P., A Family of Parallel Runge-Kutta Pairs, Computers Math. Applic., 31 (1996), 23-31.
[4] Bogacki, P. and Shampine, L. F., An Efficient Runge-Kutta (4,5) Pair, Computers Math. Applic., 32 (1996), 15-28.
[5] Cash, R. J. and Karp, A. H., A Variable Order Runge-Kutta for Initial Value Problems with Rapidly Varying Right-Hand Sides, ACM Transaction on Mathematical Software, 16 (1990), 201-222.
[6] Chen, X. and Chadam, J., Analytical and Numerical Approximations for the Early Exercise Boundary for American Put Options, Cont. Disc. and Imp. Systs., Series A: Math. Anal., 10 (2003).
[7] Chen, X. and Chadam, J., A Mathematical Analysis of the Optimal Exercise Boundary American Put Options, SIAM Journal on Mathematical Analysis, 38 (2006), 1613-1641.
[8] Chen, X., Chadam, J., Jiang, L. and Zheng, W.: Convexity of the Exercise Boundary of the American Put Option on a Zero Dividend Asset, Mathematical Finance, 18 (2008), 185-197.
[9] Company, R., Egorova, V.N. and Jdar, L., Solving American Option Pricing Models by the Front Fixing Method: Numerical Analysis and Computing, Abstract and Applied Analysis, 146745 (2014).
[10] Cox, J. C., Ross, S. A. and Rubinstein, M., Option Pricing: A Simplified Approach, Journal of Financial Economics, 7 (1979), 229-263.
[11] Dormand, J. R. and Prince, J. P., A Family of Embedded Runge-Kutta Formulae, Journal of Computational and Applied Mathematics, 6 (1980), 19-26.
[12] Fehlberg, E., Low-Order Classical Runge-Kutta Formulas with Step Size Control and their Application to Some Heat Transfer Problems, NASA Technical Report, 315 (1969).
[13] Fekete, I., Conde, S. and Shadid, J. N., Embedded Pairs for Optimal Explicit Strong Stability Preserving Runge-Kutta Methods, Journal of Computational and Applied Mathematics, 412 (2022), 114325.
[14] Gottlieb S., Shu, C. W. and Tadmore, E., Strong-Stability Preserving High-Order Time Discretization Methods, SIAM Rev., 43 (2001), 89-112.
[15] Hajipour, M. and Malek, A., Efficient High-Order Numerical Methods for Pricing Option, Computational Economics, 45 (2015), 31-47.

[16] Ketcheson, D. I., Mortenson, M., Parsani, M. and Schilling, N., More Efficient Time Integration for Fourier Pseudospectral DNS of Incompressible Turbulence, Int. J. Numer. Meth. Fluids, 92 (2020), 79C93.
[17] Kim, B. J., Ma, Y. and Choe, H. J., A Simple Numerical Method for Pricing an American Put Option, Journal of Applied Mathematics, 128025 (2013).
[18] Kim, B. J., Ma, Y. and Choe, H. J., Optimal Exercise Boundary via Intermediate Function with Jump Risk, Japan Journal of Industrial and Applied Mathematics, 34 (2017), 779-792.
[19] Lee, J. K., On a Free Boundary Problem for American Options under the Generalized BlackC-Scholes Model. Mathematics, 8 (2020a), 1563.
[20] Lee, J. K., A Simple Numerical Method for Pricing American Power Put Options, Chaos, Solitons, and Fractals, 139 (2020b).
[21] Macdougall, T. and Verner, J. H., Global Error Estimators for 7, 8 Runge-Kutta Pairs, Numerical Algorithm, 31 (2002), 215-231.
[22] Mallier, R., Evaluating Approximations to the Optimal Exercise Boundary for American Options. Journal of Applied Mathematics, 2(2002), 71-92.
[23] Mayo, A., High-order accurate Implicit Finite Difference Method for Evaluating American Options, The European Journal of Finance. 10 (2004), 212-237.
[24] Mehra M. and Patel, K. S.: Algorithm 986: A suite of Compact Finite Difference Schemes. ACM Transactions in Mathematical Softwares, 44 (2018), 1-31.
[25] Nwankwo, C. and Dai, W., Explicit RKF-Compact Scheme for Pricing Regime Switching American Options with Varying Time Step, https://arxiv.org/abs/2012.09820, (2020).
[26] Nwankwo, C. and Dai, W., An Adaptive and Explicit Fourth Order RungeCKuttaCFehlberg Method Coupled with Compact Finite Differencing for Pricing American Put Options, Japan J. Indust. Appl. Math., 38 (2021), 921-946.
[27] Nwankwo, C. and Dai, W., On the Efficiency of 5(4) RK-Embedded Pairs with High Order Compact Scheme and Robin Boundary Condition for Options Valuation, Japan J. Indust. Appl. Math., 39 (2022), 753-775.
[28] Papakostas S.N. and Papageorgiou, G.: A Family of Fifth-Order Runge-Kutta Pairs, Mathematics of Computation, 65 (1996), 1165-1181.
[29] Sari, M. and Gulen, S., Valuation of the American Put Options as a Free Boundary Problem Through a High-Order Difference Scheme, International Journal of Nonlinear Science and Numerical Solution, (2021).
[30] Simos, T. E., A Runge-Kutta Fehlberg Method with Phase-Lag of Order Infinity for Initial-Value Problems with Oscillation Solution, Computers and Mathematics with Application, 25 (1993), 95-101.
[31] Simos, T. E. and Papakaliatakis, G., Modified Runge-Kutta Verner Methods for the Numerical Solution of Initial and Boundary-Value Problems with Engineering Application, Applied Mathematical Modelling, 22 (1998), 657-670.
[32] Simos, T. E., and Tsitouras, C., Fitted Modifications of Classical Runge-Kutta Pairs of Orders 5(4), Math Meth Appl Sci., 41 (2018), 4549-4559.
[33] Tangman, D. Y. Gopaul, A. and Bhuruth, M., A Fast High-Order Finite Difference Algorithm for Pricing American Options, Journal of Computational and Applied Mathematics, 222 (2008), 17-29.
[34] Tsitouras, C., A Parameter Study of Explicit Runge-Kutta Pairs of Orders 6(5), Applied Mathematics Letter, 11 (1998), 65-69.
[35] Wang, D., Serkh, K., and Christara, C., A High-Order Deferred Correction Method for the Solution of Free Boundary Problems using Penalty Iteration with An Application to American Option Pricing, Journal of Computational and Applied Mathematics, 432 (2023), 115272.
[36] Wilkie, J. and Cetinbas, M., Variable-Stepsize Runge-Kutta for Stochastic Schrodinger Equations, Physics Letters A, 337 (2005), 166-182.
[37] William, H. P. and Saul, A. T., Adaptive Stepsize Runge-Kutta Integration, Computer in Physics, 6 (1992), 188.
[38] Wu, L., Kwok, Y.K., A Front-Fixing Method for the Valuation of American Options, J. Finance. Eng., 6 (1997), 83-97.
[39] Yambangwai, D., N. Moshkin., Deferred Correction Techniques to Construct High-Order Schemes for the Heat Equation with Dirichlet and Neumann Boundary Conditions, IAENG International Journal of Computer Science, 21 (2013).
[40] Zhao, J., Davidson, M., and Corless, R. M., Compact Finite Difference Method for Integro-Differential Equations, Applied Mathematics and Computations, 177 (2006), 271-288.

[41] Zhao, J., Highly Accurate Compact Mixed Method for Two Point Boundary Value Problem, Applied Mathematics and Computation, 188 (2007), 1402-1418.
[42] Zhao, J., Davidson, M. and Corless, R. M., Compact Finite Difference Method for American Option Pricing, Journal of Computational and Applied Mathematics, 206 (2007), 306-321.

Department of Mathematics and Statistics, University of Calgary, Calgary T2N 1N4, Canada
E-mail: chinonso.nwankwo@ucalgary.ca

Mathematics and Statistics, Louisiana Tech University, Ruston, LA 71272, USA
E-mail: dai@coes.latech.edu